Numerical evaluation of the inflationary tensor bi-spectrum using Python

A project report
submitted in partial fulfilment for the award of the degree of
B.S & M.S in Physics
by

Poruri Sai Rahul

under the guidance of

Dr. L. Sriramkumar

Department of Physics
Indian Institute of Technology Madras
Chennai 600036, India

June 2015

CERTIFICATE

This is to certify that the project titled **Numerical evaluation of the tensor bi-spectrum during power law inflation** is a bona fide record of work done by **Poruri Sai Rahul** towards the partial fulfilment of the requirements of the B.S & M.S degree in Physics at the Indian Institute of Technology, Madras, Chennai 600036, India.

(L. Sriramkumar, Project supervisor)

ACKNOWLEDGEMENTS

I cannot express in words my gratitude to Dr. L. Sriramkumar for guiding me, regarding my work and my personal life. I would also like to thank V. Sreenath and Debika Choudhury for helping me with my project and for clarifying my doubts. I would like to thank my family and my friends, especially Preeti Saryan and Malayaja Chutani, who have kept me on my toes over the last few years.

ABSTRACT

Theories of inflation provide a causal mechanism for the origin of perturbations in the early universe, perturbations which evolve and leave an imprint on the cosmic microwave background. The n-point statistics of the observed perturbations can be used to constrain various models of inflation. Most of the efforts have been to study the tensor power spectrum. In this work, I study the tensor bi-spectrum during two models of inflation, namely power law inflation and inflation driven by a quadratic potential model. The aim of this work is to construct a Python code to numerically evaluate the tensor bi-spectrum during inflation for an arbitrary triangular configuration of wavevectors.

Contents

1 Introduction **1**

1.1 Conventions and notations 2

1.2 Metric perturbations 2

1.3 Quantization of metric perturbations 4

1.4 The Bunch-Davies initial conditions 5

1.5 The tensor bi-spectrum 6

1.6 Driving inflation 7

2 Inflationary models **10**

2.1 Power law inflation 10

2.1.1 Evolution of the scalar field driving power law inflation 11

2.1.2 The tensor power spectrum during power law inflation 12

2.2 Slow roll inflation 12

2.2.1 Evolution of the scalar field during slow-roll inflation 14

2.2.2 The tensor power spectrum during slow-roll inflation 14

2.2.3 The tensor bi-spectrum during slow-roll inflation 16

3 Numerical results **18**

3.1 Numerical evaluation of the inflaton 18

3.2 Numerical evaluation of the tensor power spectrum 21

3.3 Numerical evaluation of the tensor bi-spectrum 24

3.3.1 Equilateral limit 25

3.3.2 Squeezed limit 31

3.3.3 Triangular configuration of wavevectors 34

4 Summary **38**

Appendix A Python code : Arbitrary triangular configuration of wavevectors **42**

List of Figures

3.1 Numerical estimate of the scalar field ϕ as a function of N in power law inflation. 20
3.2 Numerical estimate of the Hubble parameter H as a function of N in power law inflation. 20
3.3 Numerical estimate of the scalar field ϕ as a function of N in inflation driven by quadratic potential model. 21
3.4 Numerical estimate of the Hubble parameter H as a function of N in inflation driven by quadratic potential model. 22
3.5 Numerical estimate of the tensor power spectrum $\mathcal{P}_{\mathrm{T}}$ as a function of k in power law inflation. 23
3.6 Numerical estimate of the tensor power spectrum $\mathcal{P}_{\mathrm{T}}$ as a function of k in inflation driven by quadratic potential model. 24
3.7 Numerical estimate of $\mathcal{G}$ as a function of k in the equilateral limit in power law inflation. 26
3.8 Numerical estimate of the tensor bi-spectrum $G_{\gamma\gamma\gamma}$ as a function of k in the equilateral limit in power law inflation. 27
3.9 Numerical estimate of the invariant $k^6 G_{\gamma\gamma\gamma}$ as a function of k in the equilateral limit in power law inflation. 28
3.10 Numerical estimate of the non-Gaussianity parameter h_{NL} as a function of k in the equilateral limit in power law inflation. 29
3.11 Numerical estimate of $\mathcal{G}$ as a function of k in the equilateral limit in inflation driven by quadratic potential model. 29
3.12 Numerical estimate of the tensor bi-spectrum $G_{\gamma\gamma\gamma}(k)$ as a function of k in the equilateral limit in inflation driven by quadratic potential model. 30

3.13 Numerical estimate of the invariant $k^6 G_{\gamma\gamma\gamma}$ as a function of k in the equilateral limit in inflation driven by quadratic potential model. 30
3.14 Numerical estimate of the non-Gaussianity parameter h_{NL} as a function of k in the equilateral limit in inflation driven by quadratic potential model. 31
3.15 Numerical estimate of the tensor bi-spectrum $G_{\gamma\gamma\gamma}$ as a function of k in the squeezed limit in power law inflation. 32
3.16 Numerical estimate of the invariant $k_0^{3/2} k^{3/2} G_{\gamma\gamma\gamma}(k)$ as a function of k in the squeezed limit in power law inflation. 33
3.17 Numerical estimate of the non-Gaussianity parameter h_{NL} as a function of k in the squeezed limit in power law inflation. 33
3.18 Numerical estimate of the tensor bi-spectrum $G_{\gamma\gamma\gamma}(k)$ as a function of k in the squeezed limit in inflation driven by quadratic potential model. 34
3.19 Numerical estimate of the invariant $k_0^{3/2} k^{3/2} G_{\gamma\gamma\gamma}(k)$ as a function of k in the squeezed limit in inflation driven by quadratic potential model. 35
3.20 Numerical estimate of the non-Gaussianity parameter h_{NL} as a function of k in the squeezed limit in inflation driven by quadratic potential model. 35
3.21 Density plot of the numerical estimates of the non-Gaussianity parameter h_{NL} as a function of k for a triangular configuration of wavevectors in power law inflation. 36
3.22 Density plot of the non-Gaussianity parameter h_{NL} as a function of k for a triangular configuration of wavevectors in inflation driven by quadratic potential model. 37

Chapter 1

Introduction

Inflation refers to a period of rapid expansion in the early universe and the theory of inflation was proposed to overcome a few of the drawbacks of the conventional hot big bang model of the universe, the flatness problem and the horizon problem to name a few. Inflation also provides a causal mechanism for the generation of perturbations in the universe, perturbations which evolved into the large scale structure of the universe. From an observational perspective, the inhomogenities in the early universe leave an imprint as anisotropies on the cosmic microwave background (CMB) and studying the CMB, specifically the n-point statistics of perturbations, will help us constrain numerous inflationary models. The two-point statistic refers to the power spectrum of perturbations and the three-point statistic refers to the bi-spectrum of perturbations. In this work, I will study the tensor bi-spectrum, the simplest of the three-point functions to study.

This thesis presents a study of the tensor bi-spectrum, $G_{\gamma\gamma\gamma}(\mathbf{k}_1, \mathbf{k}_2, \mathbf{k}_3)$, and the non-Gaussianity parameter, h_{NL}. It is organized as follows. In this chapter, I give a brief introduction to inflation and why scalar fields are needed to drive inflation. I also introduce the conditions imposed on a scalar field that drives inflation. I will discuss linear perturbation theory and tensor perturbations in the metric. I will discuss how the scale factor, $a(t)$, the scalar field, ϕ, and the potential driving the scalar field, $V(\phi)$, are related to each other. In the next chapter, I will discuss how we can solve the equation governing the evolution of the tensor perturbations after we obtain solutions for the evolution of the scalar field driving inflation. After obtaining solutions for the evolution of the tensor perturbations, I will discuss how the tensor bi-spectrum, $G_{\gamma\gamma\gamma}(\mathbf{k}_1, \mathbf{k}_2, \mathbf{k}_3)$, can be evaluated. In the third chapter,

I will discuss the numerical methods implemented to solve for the scalar field ϕ, the tensor perturbations h_k, the tensor bi-spectrum $G_{\gamma\gamma\gamma}(\mathbf{k}_1, \mathbf{k}_2, \mathbf{k}_3)$ and the non-Gaussianity parameter h_{NL}.

1.1 Conventions and notations

I shall work in $(3 + 1)$ dimensions and I shall adopt the metric signature $(-, +, +, +)$. Latin indices, with the exception of k which represents wavevectors, represent spatial coordinates whereas greek indices denote all spacetime coordinates. Planck mass is defined as $M_{Pl} = (8\pi G)^{-1/2}$. t refers to cosmic time and an overdot refers to differentiation with respect to cosmic time whereas η refers to conformal time and an overprime represents differentiation with respect to conformal time. For convenience with the numerics, we measure the duration of inflation not in terms of cosmic time or conformal time but in terms of e-folds N, where N is defined as

$$N = \ln\left(\frac{a(t)}{a_0}\right), \tag{1.1}$$

a_0 is the scale factor when inflation started and $a(t)$ is the scale factor when inflation ends.

1.2 Metric perturbations

Inhomogenities in the Cosmic Microwave Background have been measured to be one part in 10^5 [1, 2] and given the expanding nature of our universe, it can be inferred that they were much smaller at earlier epochs. Therefore, we can study the generation and evolution of such anisotropies in the universe using linear perturbation theory.

The perturbations in a Friedmann background can be classified as scalar, vector and tensor according to their behaviour under local rotation of spatial coordinates on hyper surfaces of constant time. The perturbations that remain invariant under rotations are classified as scalar. In fact, scalar perturbations are largely responsible for the anisotropy we see in our universe. Vector and tensor perturbations behave as vectors and tensors under local rotations. Rotational velocity fields generate vector perturbations and are therefore also referred to as Vorticity modes and the tensor perturbations describe gravitational waves.

(Refs. [3, 4, 5, 6, 7, 8, 9, 10, 11, 12] can be studied for a better understanding of cosmological linear perturbation theory.) I shall restrict myself to tensor perturbations of the metric for the scope of this work.

The metric tensor governing a Friedmann universe describes a homogeneous and isotropic universe, which is not a valid assumption under the presence of perturbations. We can therefore choose to work in a number of coordinate systems under the condition that they reduce to the standard Friedmann line element in the limit when the perturbations vanish. We shall represent the tensor perturbations in the metric as

$$\mathrm{d}s^2 = -\mathrm{d}t^2 + h_{ij}(t, \mathbf{x})\mathrm{d}x^i\mathrm{d}x^j, \tag{1.2}$$

where the tensor perturbations are characterized by the transverse, traceless matrix γ_{ij}, *i.e.* they satisfy the conditions $\gamma_{ii} = \mathrm{d}_i\gamma_{ij} = 0$, and is given by

$$h_{ij} = a^2(t)\left[e^{\gamma(t,\mathbf{x})}\right]_{ij}. \tag{1.3}$$

Similar to how we characterized the perturbations, we can characterize the sources which give rise to them, namely the stress-energy tensor. Like the metric tensor, the stress-energy tensor is a two tensor and therefore, perturbations in the stress-energy tensor can also be classified into scalar, vector and tensor components. The decomposition theorem dictates that scalar, vector and tensor perturbations are decoupled and can therefore be studied independent of one another. Therefore, a scalar field driving inflation is a scalar source that gives rise to scalar perturbations, velocity fields with Vorticity are vector sources that give rise to vector perturbations and having eliminated the scalar and vector contributions, anisotropic stresses constitute a tensor source that give rise to tensor perturbations.

The perturbed metric, say $\delta g_{\mu\nu}$, can be used to derive the perturbed Einstein tensors, which can then be related to the perturbed stress-energy tensor, say $\delta T_{\mu\nu}$, giving rise to the Einstein's equations which govern the evolution of the metric perturbations. Under these assumptions, the perturbed Einstein tensor governing the tensor perturbations corresponding to the metric described in Eqn. (1.2) is given by

$$\delta G^i_j = -\left(\frac{1}{2}\right)\left(\ddot{\gamma}_{ij} + 3H\dot{\gamma}_{ij} - \frac{1}{a^2}\nabla^2\gamma_{ij}\right), \tag{1.4}$$

after imposing the condition that γ_{ij} is a transverse and traceless matrix. In the absence of anisotropic stresses i.e if $\delta T^i_j = 0$, we get that

$$\ddot{\gamma} + 3H\dot{\gamma} - \left(\frac{1}{a^2}\right)\nabla^2\gamma = 0. \tag{1.5}$$

which is the equation governing the evolution of tensor perturbations across cosmic time t. The above equation can be rewritten in terms of conformal time η as

$$\gamma^{''} + 2\mathcal{H}\gamma^{'} - \nabla^2\gamma = 0, \tag{1.6}$$

where $\mathcal{H} = a^{'}/a$.

1.3 Quantization of metric perturbations

As I had mentioned earlier, understanding the n-point statistics of the perturbations will help us constrain numerous inflationary models. Therefore, we would like to understand the behaviour of the tensor perturbations in Fourier space. Eqn. (1.6) that governs the evolution of the tensor perturbations in conformal time, η, can be rewritten in Fourier space as

$$g_k^{''} + 2\mathcal{H}g_k^{'} + k^2 g_k = 0. \tag{1.7}$$

The homogeneity of the Friedmann background allows us to quantize the tensor perturbations. Upon quantization, we can write the tensor perturbation, $\hat{\gamma}$, in terms of it's Fourier component, $g_k(\eta)$, as

$$\hat{\gamma}_{ij}(\eta, \mathbf{x}) = \sum_s \int \frac{\mathrm{d}^3\mathbf{k}}{(2\pi)^{3/2}}\left[\hat{a_k}^s \varepsilon^s_{ij}(\mathbf{k}) g_k(\eta) e^{i\mathbf{k}\cdot\mathbf{x}} + \hat{a_k}^{s^\dagger} \varepsilon^{s*}_{ij}(\mathbf{k}) g^*_k(\eta) e^{-i\mathbf{k}\cdot\mathbf{x}}\right], \tag{1.8}$$

where the creation and annihilation operators, $\hat{a}^s_k$ and $\hat{a}^{s^\dagger}_k$, follow the standard commutation relations. $\varepsilon^s_{ij}(\mathbf{k})$ denotes the polarization tensor of tensor perturbations, where s denotes their helicity and it satisfies the conditions $\varepsilon^s_{ii}(\mathbf{k}) = k_i\varepsilon^s_{ij}(\mathbf{k}) = 0$ given the transverse and

traceless nature of the tensor perturbations. As we are working in the linear order in perturbations, the two point function of the quantum field, $\hat{\gamma}$, can be used to characterize the power spectrum of the tensor perturbations. The power spectrum of the tensor perturbations $\mathcal{P}_T(k)$ is defined as

$$\langle \hat{\gamma}_{ij}^{\mathbf{k}}(\eta)\hat{\gamma}_{mn}^{\mathbf{k}'}(\eta)\rangle = \frac{(2\pi)^2}{2k^3}\frac{\Pi_{ij,mn}^{\mathbf{k}}}{4}\mathcal{P}_T(k)\delta^{(3)}(\mathbf{k}+\mathbf{k}'), \tag{1.9}$$

where the quantity $\Pi_{ij,mn}^{\mathbf{k}}$ is given by

$$\Pi_{ij,mn}^{\mathbf{k}} = \sum_s \varepsilon_{ij}^s(\mathbf{k})\varepsilon_{mn}^{s*}(\mathbf{k}). \tag{1.10}$$

The vaccum state $|0\rangle$ is defined as $\hat{a}_{\mathbf{k}}^s|0\rangle = 0\ \forall\ \mathbf{k}$ and s. Using Eqs. (1.8) and (1.9) and the assumption that the vacuum state $|0\rangle$ is the initial quantum state of the perturbations, we can obtain the tensor power spectrum as

$$\mathcal{P}_{\rm T}(k) = 4\frac{k^3}{2\pi^2}|g_k|^2. \tag{1.11}$$

1.4 The Bunch-Davies initial conditions

We need to understand the initial conditions from which the tensor perturbations evolve in order to arrive at a complete analytical solution to the problem at hand. On individual modes, we impose the initial conditions when they are well within the Hubble radius i.e when $\eta \to -\infty$ or $(k/aH) \gg 1$. In this sub-Hubble limit, the curvature of space-time can be neglected. Further, upon imposing the condition that the solution u_k contain positive frequency modes, we obtain a solution to the Eqn. (2.8) in the sub-Hubble limit as

$$\lim_{(k/aH)\to\infty} u_k(\eta) \to \left(\frac{1}{\sqrt{2k}}\right)\mathrm{e}^{-ik\eta}, \tag{1.12}$$

where $u_k = M_{Pl}\ a\ g_k/\sqrt{2}$.

1.5 The tensor bi-spectrum

The moments of primordial perturbations can be used to understand their statistical properties. The variance or the power spectrum of the primordial perturbations would have contained all of it's statistical properties if they were Gaussian. However, non-Gaussianities in the primordial perturbations would manifest either as non-zero odd moments or as the even moments taking a different form. Hence, non-zero three point functions of the primordial perturbations would be the first evidence of non-Gaussianity. We adopt the so-called Maldacena formalism as it is the most complete formalism to calculate the three-point functions generated during inflation amongst different approaches [15]. In this section, we will only concentrate on the three-point function involving tensors.

The tensor bi-spectrum in Fourier space, $G_{\gamma\gamma\gamma}^{m_1n_1m_2n_2m_3n_3}(\mathbf{k}_1, \mathbf{k}_2, \mathbf{k}_3)$ evaluated towards the end of inflation at conformal time, say η_e, is defined as [15, 16, 17, 18, 19]

$$\langle \hat{\gamma}_{m_1n_1}^{\mathbf{k}_1}(\eta_e)\hat{\gamma}_{m_2n_2}^{\mathbf{k}_2}(\eta_e)\hat{\gamma}_{m_3n_3}^{\mathbf{k}_3}(\eta_e)\rangle = (2\pi)^{-3/2}G_{\gamma\gamma\gamma}^{m_1n_1m_2n_2m_3n_3}(\mathbf{k}_1, \mathbf{k}_2\mathbf{k}_3)\delta^{(3)}(\mathbf{k}_1 + \mathbf{k}_2 + \mathbf{k}_3), \quad (1.13)$$

where $\gamma_{mn}^{\mathbf{k}}$ represents the tensor perturbation γ_{mn} in Fourier space. We can arrive at the tensor three-point function using the action governing the tensor perturbations and the standard rules of perturbative quantum field theory [15, 16, 17, 18, 19]. Using Maldecena's approach, we can obtain a cubic order action of the form,

$$S_{\gamma\gamma\gamma}^3[\gamma_{ij}] = \frac{1}{2}\int \mathrm{d}\eta \int \mathrm{d}^3\mathbf{x}\left[\frac{a^2}{2}\gamma_{lj}\gamma_{im}\partial_l\partial_m\gamma_{ij} - \frac{a^4}{4}\gamma_{ij}\gamma_{lm}\partial_l\partial_m\gamma_{ij}\right]. \quad (1.14)$$

The interaction Hamiltonian corresponding to the above action is needed to evaluate the three-point correlation function using the methods of quantum field theory. At the cubic order, it can be shown that $H_{int} = -L_{int}$, where H_{int} is the interaction Hamiltonian and L_{int} is the interaction Lagrangian [15, 16, 17, 18, 19]. The tensor bi-spectrum $G_{\gamma\gamma\gamma}^{m_1n_1m_2n_2m_3n_3}(\mathbf{k}_1, \mathbf{k}_2, \mathbf{k}_3)$ can be expressed in terms of the Hamiltonian $\hat{H}_{\gamma\gamma\gamma}$ as [17, 19, 20]

$$\langle \hat{\gamma}_{m_1n_1}^{\mathbf{k}_1}(\eta_e)\hat{\gamma}_{m_2n_2}^{\mathbf{k}_2}(\eta_e)\hat{\gamma}_{m_3n_3}^{\mathbf{k}_3}(\eta_e)\rangle = -i\int_{\eta_i}^{\eta_e}\mathrm{d}\eta\langle[\hat{\gamma}_{m_1n_1}^{\mathbf{k}_1}(\eta_e)\hat{\gamma}_{m_2n_2}^{\mathbf{k}_2}(\eta_e)\hat{\gamma}_{m_3n_3}^{\mathbf{k}_3}(\eta_e), \hat{H}_{\gamma\gamma\gamma}(\eta)]\rangle. \quad (1.15)$$

The tensor bi-spectrum $G_{\gamma\gamma\gamma}^{m_1n_1m_2n_2m_3n_3}(\mathbf{k}_1,\mathbf{k}_2,\mathbf{k}_3)$, calculated in perturbative vaccum, can be written as [15, 17, 19, 20]

$$
\begin{aligned}
&G_{\gamma\gamma\gamma}^{m_1n_1m_2n_2m_3n_3}(\mathbf{k}_1,\mathbf{k}_2,\mathbf{k}_3) = \\
&M_{Pl}^2\left[\left(\Pi_{m_1n_1,ij}^{\mathbf{k}_1}\Pi_{m_2n_2,im}^{\mathbf{k}_2}\Pi_{m_3n_3,lj}^{\mathbf{k}_3} - \frac{1}{2}\Pi_{m_1n_1,ij}^{\mathbf{k}_1}\Pi_{m_2n_2,ml}^{\mathbf{k}_2}\Pi_{m_3n_3,ij}^{3}\right)k_{1m}k_{1l} + \text{ five permutations}\right] \\
&\times\left[g_{k1}(\eta_e)g_{k2}(\eta_e)g_{k3}(\eta_e)\mathcal{G}_{\gamma\gamma\gamma} + \text{ complex conjugate}\right],
\end{aligned}
$$

where the quantities $\mathcal{G}$ is given by [18, 19]

$$\mathcal{G}_{\gamma\gamma\gamma}(\mathbf{k}_1,\mathbf{k}_2,\mathbf{k}_3) = \frac{-i}{4}\int_{\eta_i}^{\eta_e}\mathrm{d}\eta a^2 h_{\mathbf{k}_1}^* h_{\mathbf{k}_2}^* h_{\mathbf{k}_3}^*. \tag{1.16}$$

1.6 Driving inflation

In a spatially flat, smooth Friedmann universe, the line element that describes the universe can be written as

$$\mathrm{d}s^2 = \mathrm{d}t^2 - a^2(t)\mathrm{d}\mathbf{x}^2 = a^2(\eta)\left(\mathrm{d}\eta^2 - \mathrm{d}\mathbf{x}^2\right), \tag{1.17}$$

and for such a line element, the Einstein's equations can be rewritten as the following two Friedmann equations

$$\left(\frac{\dot{a}}{a}\right)^2 = H^2 = \left(\frac{8\pi G}{3}\right)\rho, \tag{1.18}$$

$$\left(\frac{\ddot{a}}{a}\right) = \dot{H} + H^2 = -\left(\frac{4\pi G}{3}\right)(\rho + 3p), \tag{1.19}$$

where ρ and p denote the energy density and the pressure of the field driving the change and $H = \dot{a}/a$ is the Hubble parameter. A necessary condition to solve the horizon problem and to achieve inflation on the scale factor $a(t)$ is

$$\ddot{a} > 0. \tag{1.20}$$

From Eqns. (1.19) and (1.20), it is straight forward to notice that

$$\rho + 3p < 0, \tag{1.21}$$

is a necessary condition for a field that drives inflation. We know that a matter field has $p = 0$ and that a radiation field has $p = \rho/3$, neither of which satisfy the above condition. We therefore invoke the presence of a scalar field ϕ, itself driven by a potential $V(\phi)$, to drive inflation. A scalar field that drives inflation is also referred to as an Inflaton.

We can write the action, $S[\phi]$, for such a scalar field and the corresponding stress-energy tensor $T_{\mu\nu}$ as

$$S[\phi] = \int \mathrm{d}^4x\sqrt{-g}\left[\left(\frac{1}{2}\right)\left(\partial^\lambda\phi\partial_\lambda\phi\right) - V(\phi)\right], \tag{1.22}$$

$$T^\mu_\nu = \partial^\mu\phi\partial_\nu\phi - \delta^\mu_\nu\left[\left(\frac{1}{2}\right)\left(\partial^\lambda\phi\partial_\lambda\phi\right) - V(\phi)\right]. \tag{1.23}$$

From Eqn. (1.22) defining the action, $S[\phi]$, for a scalar field ϕ, we can derive the equation of motion for the scalar field to be

$$\ddot{\phi} + 3H\dot{\phi} + V_\phi = 0, \tag{1.24}$$

where $V_\phi = \mathrm{d}V/\mathrm{d}\phi$.

We can also arrive at solutions to the scalar field, ϕ, and the potential, $V(\phi)$, using the stress-energy tensor, T^μ_ν, defined in Eqn. (1.23) and the Friedmann equations defined in Eqns. (1.18) and (1.19). From Eqn. (1.23), we can write the individual components of the stress-energy tensor as

$$T^0_0 = \left(\frac{\dot{\phi}^2}{2}\right) + V(\phi) = \rho, \tag{1.25}$$

$$T^i_j = -\left[\left(\frac{\dot{\phi}^2}{2}\right) - V(\phi)\right]\delta^i_j = -p\delta^i_j. \tag{1.26}$$

Using the definitions for energy density ρ and the pressure p from Eqs. (1.25) and (1.26), we can rewrite Eqs. (1.18) and (1.19) defining the Hubble parameter and the evolution of the Hubble parameter in cosmic time t as

$$\dot{H} = \frac{-\dot{\phi}^2}{2M_{Pl}^2}, \tag{1.27}$$

$$H^2 = \left(\frac{1}{3M_{Pl}^2}\right)\left(\frac{\dot{\phi}^2}{2} + V\right). \tag{1.28}$$

We can also rewrite Eqn. (1.27) and (1.28) to express the scalar field ϕ and the potential V in terms of the Hubble parameter and the first derivative of the Hubble parameter in terms of cosmic time, t, as

$$\phi(t) = \sqrt{2}\int dt\sqrt{-\dot{H}}, \tag{1.29}$$

$$V(t) = 3H^2 + \dot{H}. \tag{1.30}$$

Chapter 2

Inflationary models

Numerous models have been proposed to solve the horizon problem. In this chapter, I will specifically discuss power law inflation and slow-roll inflation. I will discuss the form of the scalar field driving inflation and the solution of the equation governing the evolution of the tensor perturbations and the analytic form of the tensor power spectrum in both cases. Further, I will discuss the analytic form of the tensor bi-spectrum during slow-roll inflation.

2.1 Power law inflation

Power law inflation is one of many models of inflation where inflation is being driven by a single scalar field. During power law inflation, we assume that the scale factor, $a(t)$, has a power law dependence on cosmic time t, namely

$$a(t) = a_0 t^q. \tag{2.1}$$

We can be rewrite the above equation to obtain the evolution of the scale factor in terms of conformal time, η, as

$$a(\eta) = \left(-\bar{\mathcal{H}}\eta\right)^{(\gamma+1)}, \tag{2.2}$$

where $\bar{\mathcal{H}}$ and γ are given by

$$\bar{\mathcal{H}} = a_0^{1/q}(q-1) \ \text{ and } \gamma = -\left(\frac{2q-1}{q-1}\right). \tag{2.3}$$

2.1.1 Evolution of the scalar field driving power law inflation

Using the scale factor given by Eqn. (2.1), we can rewrite the Eqns. (1.29) and (1.30) that define the scalar field, ϕ, and the potential, V, in terms of the Hubble parameter, H, and it's first derivative with respect to cosmic time, $\dot{H}$, as

$$\phi(t) = \sqrt{(2q)} \ln \left[t \sqrt{\left(\frac{V_0}{(3q-1)q} \right)} \right], \tag{2.4}$$

$$V(\phi) = V_0 \ \exp \left[-\phi \sqrt{\left(\frac{2}{q} \right)} \right]. \tag{2.5}$$

Further, for convenience in numerical evaluation, we can rewrite the scalar field, ϕ, and the Hubble parameter, H, in terms of e-fold N as

$$\phi(N) = \sqrt{\left(\frac{2}{q} \right)} N - \sqrt{(2q)} \ln t_0, \tag{2.6}$$

$$H(N) = H_0 \exp^{-N/q}, \tag{2.7}$$

where $t_0 = \sqrt{((3q-1)q/V_0)}$.

Having solved the background equations that govern the evolution of the scalar field during inflation, we can now attempt to solve the equation governing the evolution of tensor perturbations. We can rewrite Eqn. (1.6) governing the evolution of tensor perturbations in conformal time, η, by substituting $g_k = (u_k/a)$ as

$$u_k'' + \left[k^2 - \left(\frac{a''}{a} \right) \right] u_k = 0, \tag{2.8}$$

and the power spectrum governing tensor perturbations, namely Eqn. (1.11), can be rewritten as

$$\mathcal{P}_{\rm T}(k) = 4 \left(\frac{k^3}{2\pi^2} \right) |h_k|^2 = 4 \left(\frac{k^3}{2\pi^2} \right) \left(\frac{|u_k|}{a} \right)^2. \tag{2.9}$$

2.1.2 The tensor power spectrum during power law inflation

Armed with the analytic solution to the background driving inflation and the initial conditions imposed on the tensor perturbations, we can attempt to solve the Eqn. (1.7) governing the evolution of tensor perturbations in fourier space to obtain the power spectrum of tensor perturbations. Substituting the scale factor given by Eqn. (2.1) in the Eqn. (2.8), we can arrive at a solution satisfying the initial conditions defined in Eqn. (1.12) as

$$u_k(\eta) = \left(\frac{-\pi\eta}{4}\right)^{1/2} \mathrm{e}^{i[\nu+(1/2)](\pi/2)} \mathrm{H}_{\nu}^{(1)}(-k\eta), \tag{2.10}$$

where $\nu = [\gamma + (1/2)]$ and $\mathrm{H}_{\nu}^{(1)}$ is the Hankel function of the first kind and of order ν [13]. In the super-Hubble limit (i.e as $(-k\eta \to 0)$), we can approximate the Hankel function to

$$\mathrm{H}_{\nu}^{(1)}(z) \sim -(i/\pi)\Gamma(\nu)\left(\frac{z}{2}\right)^{(-\nu)}, \tag{2.11}$$

where $\Gamma(\nu)$ is a Gamma function. In the super-Hubble limit, u_k and a have the same behaviour and therefore, the tensor perturbation h_k reach a constant value, allowing us to obtain the tensor power spectrum in the super-Hubble limit as

$$\mathcal{P}_{\mathrm{T}}(k) = A_T \bar{\mathcal{H}}^2 \left(\frac{k}{\bar{\mathcal{H}}}\right)^{2(\gamma+2)}, \tag{2.12}$$

where

$$A_T = \left[\frac{1}{\pi^3}\right]\left(\frac{|\Gamma(\nu)|^2}{2^{(2\gamma+1)}}\right). \tag{2.13}$$

2.2 Slow roll inflation

We have previously seen that $(\rho + 3p) < 0$ is a necessary condition for inflation to take place. Using the definitions of ρ and p from Eqn. (1.25) and Eqn. (1.26), we can restate the above the condition as $\dot{\phi}^2 < V(\phi)$. However, if $\dot{\phi}^2 << V(\phi)$, Inflation is guaranteed to take place. We can interpret the above condition as the field slowly rolling down the potential, $V(\phi)$. Moreover, using the above condition and Eqn. (3.2), we can ensure that inflation occurs for a sufficiently long time, provided $\ddot{\phi} << 3H\dot{\phi}$. These two conditions on the first and second derivative of the scalar field, phi, lead to the slow-roll approximation,

using which we can construct analytical solutions for the evolution of the background and the evolution of tensor perturbations.

The slow-roll condition is quantified using slow-roll parameters and two types of slow-roll parameters are often considered in literature, namely potential slow-roll parameters and Hubble slow-roll parameters. We will only be working with the Hubble slow-roll parameters. The Eqn. (1.27) that relates the evolution of the scalar field to the derivative of the Hubble parameter, $\dot{H}$, can be rewritten as

$$\dot{\phi} = -2M_{Pl}^2 H_\phi, \tag{2.14}$$

where $H_\phi = \mathrm{d}H/\mathrm{d}\phi$. This expression can be used to rewrite the Eqn. (1.28) that relates the Hubble parameter, H, it's derivative, $\mathrm{d}H/\mathrm{d}\phi$, and the potential, $V(\phi)$, as

$$H_\phi^2 - \frac{3H^2}{2M_{Pl}^2} = -\frac{V}{2M_{Pl}^4}, \tag{2.15}$$

The above equation is referred to as the Hamilton-Jacobi formulation of inflation. Considering the Hubble parameter, H, to be a function of the scalar field, ϕ, we can define the dimensionless Hubble slow-roll parameters ε_H and δ_H as

$$\varepsilon_H = 2M_{Pl}^2 \left(\frac{H_\phi}{H}\right)^2 \delta_H = 2M_{Pl}^2 \left(\frac{H_{\phi\phi}}{H}\right) \tag{2.16}$$

where $H_{\phi\phi} = \mathrm{d}^2H/\mathrm{d}\phi^2$. Using Eqns. (3.2), (2.14) and (2.15), we can rewrite the two Hubble slow-roll parameters as

$$\varepsilon_H = -\left(\frac{\dot{H}}{H^2}\right), \delta_H = \varepsilon_H - \left(\frac{\dot{\varepsilon_H}}{2H\varepsilon_H}\right). \tag{2.17}$$

Note that conditions on the Hubble slow-roll parameters ε_H and δ_H correspond to constraining the kinetic energy of the scalar field and the acceleration of the scalar field, respectively. Specifically, kinetic energy of the scalar field can be neglected if $\varepsilon_H << 1$ and the acceleration of the scalar field can be ignored in comparison to the term involving the velocity, $\dot{\phi}$, if $\delta_H << 1$.

2.2.1 Evolution of the scalar field during slow-roll inflation

Using the above definitions of the slow-roll parameters, let us now arrive at an analytic solution to the evolution of the scalar field. We can rewrite Eqn. (3.2), the equation governing the evolution of the scalar field. and Eqn. (1.28) in terms of the slow-roll parameters as

$$H^2\left(1-\frac{\varepsilon_H}{3}\right)=\frac{V}{3M_{Pl}^2}, \tag{2.18}$$

$$3H\dot{\phi}\left(1-\frac{\delta_H}{3}\right)=-V_\phi. \tag{2.19}$$

In the slow-roll approximation, $\varepsilon_H << 1$ and $\delta_H << 1$, the above equations can be rewritten as

$$H^2=\frac{V}{3M_{Pl}^2}, \tag{2.20}$$

$$3H\dot{\phi}=-V_\phi. \tag{2.21}$$

The above equations can be integrated trivially to arrive at an analytic solutions to evolution of the scalar field, ϕ. We can look at a general set of models the potential, $V(\phi)$, where is defined as $V(\phi)=V_0\phi^n$. These set of models are classified as 'large-field' models. For such as form of the potential function, the analytic solution to the scalar field is given by

$$\phi^{(4-n)/2)}(t)=\phi_i^{(4-n)/2)}+\sqrt{\frac{V_0}{3}}\left(\frac{n(n-4)}{2}\right)M_{Pl}(t-t_i), \tag{2.22}$$

$$\phi(t)=\phi_i\exp^{-4M_{Pl}\sqrt{V_0/3}(t-t_i)}, \tag{2.23}$$

where the first solution is when $n\neq 4$ and the second when $n=4$.

2.2.2 The tensor power spectrum during slow-roll inflation

The two Hubble slow-roll parameters, ε_H and δ_H, can be rewritten in terms of the conformal time coordinate, η, as

$$\varepsilon_H = 1 - \left(\frac{\mathcal{H}'}{\mathcal{H}^2}\right), \delta_H = \varepsilon_H - \left(\frac{\varepsilon_H'}{2\mathcal{H}\varepsilon_H}\right). \tag{2.24}$$

Further, using the first Hubble slow-roll parameter, ε_H, we can establish that

$$\left(\frac{a''}{a}\right) = \mathcal{H}^2(2 - \varepsilon_H). \tag{2.25}$$

In order to arrive at an analytic solution to the evolution of the tensor perturbations using the Eqn. (1.5), we need to be able to write $\mathcal{H}$ in terms of conformal time η. We can rewrite the first of the two equations in Eqn. (2.24) as

$$\eta = -\int \left(\frac{1}{1-\varepsilon_H}\right) \mathrm{d}\left(\frac{1}{\mathcal{H}}\right), \tag{2.26}$$

Under the slow-roll approximation, $\varepsilon_H << 1$, the above integral becomes trivial and leads to

$$\mathcal{H} = -\left[\frac{1}{(1-\varepsilon_H})\eta\right]. \tag{2.27}$$

Using the above expression for $\mathcal{H}$ in terms of the conformal time, η, we can rewrite the Eqn. (2.25) as

$$\left(\frac{a''}{a}\right) = \left(\frac{2+3\varepsilon_H}{\eta^2}\right), \tag{2.28}$$

where we assumed the slow-roll approximation and neglected the higher orders of ε_H. We can now solve the Eqn. (2.8). We can clearly see that the solutions to the equation will be Hankel functions [14], similar to the solutions in the power law case, of order, ν,

$$\nu = \left[\left(\frac{3}{2}\right) + \varepsilon_H\right]. \tag{2.29}$$

The tensor power spectrum can now be evaluated in the super-Hubble limit, i.e $-k\eta \to 0$, by expanding the Hankel function about the origin, as

$$\mathcal{P}_T(k) = \left(\frac{2H^2}{\pi^2 M_{Pl}^2}\right)\left[\frac{|\Gamma(\nu)|}{\Gamma(3/2)}\right]^2 2^{(2\nu-3)}(1-\varepsilon_H)^{(2\nu-1)}, \tag{2.30}$$

where we assumed that $-k\eta = (1-\varepsilon_H)^{-1}$. In the slow-roll approximation, the tensor power spectrum evaluated when the modes cross the Hubble radius can be approximated at the leading order as

$$\mathcal{P}_T(k) = \left(\frac{8}{2M_{Pl}^2}\right)\left(\frac{H}{2\pi}\right)^2_{k=aH}. \tag{2.31}$$

2.2.3 The tensor bi-spectrum during slow-roll inflation

Having defined the tensor bi-spectrum, let us evaluate the tensor bi-spectrum in slow roll inflation. The first two slow roll parameters, namely ϵ_1 and ϵ_2, are constant at the leading order in the slow approximation. We can assume that the scale factor as well as the tensor perturbation mode, h_k, are given by their de Sitter forms. By setting the slow roll parameters in the index, ν, of the Hankel function to zero, we can obtain the de Sitter limit of the tensor perturbation modes as

$$h_k(\eta) = \frac{\sqrt{2}}{M_{Pl}}\frac{iH_0}{\sqrt{2k^3}}(1+ik\eta)e^{-ik\eta}. \tag{2.32}$$

The tensor bi-spectrum can now be estimated by simply substituting the above form of h_k and evaluating the integral in Eqn. (1.16) from $\eta_i = -\infty$ to $\eta_e = 0$.

$$\begin{aligned}\mathcal{G}_{\gamma\gamma\gamma}(\mathbf{k}_1,\mathbf{k}_2,\mathbf{k}_3) &= \frac{-i}{4}\frac{1}{H_0^2}\left(\frac{-iH_0}{M_{Pl}}\right)^3\frac{1}{\sqrt{k_1^3k_2^3k_3^3}}\int_{\eta_i}^{\eta_e}\mathrm{d}\eta\frac{1}{\eta^2}(1-ik_1\eta)(1-ik_2\eta)(1-ik_3\eta)e^{ik_T\eta}\\ &= \frac{-i}{4}\frac{1}{H_0^2}\left(\frac{-iH_0}{M_{Pl}}\right)^3\frac{1}{\sqrt{k_1^3k_2^3k_3^3}}\int_{\eta_i}^{\eta_e}\mathrm{d}\eta\frac{1}{\eta^2}\left[-1+ik_T\eta+(k_1k_2+k_2k_3+k_3k_1)\eta^2-ik_1k_2k_3\eta^3\right]e^{ik_T\eta},\end{aligned}$$

where $k_T = k_1 + k_2 + k_3$. As you can see, the above integrand can be separated into four terms with different powers of η. While the η^0 and η^1 are straight forward to integrate, it should be noted that the η^{-2} and η^{-1}terms should be integrated together, giving rise to a term similar to$e^{-\eta}/\eta$. Together with the complex conjugate term, this term can be converted into a $\sin\eta/\eta$ term and set to 1. We can finally obtain the tensor bi-spectrum to be

$$G_{\gamma\gamma\gamma}^{m_1n_1m_2n_2m_3n_3}(\mathbf{k}_1,\mathbf{k}_2,\mathbf{k}_3) =$$
$$\frac{H_0^4}{2M_{Pl}^4}\frac{1}{k_1^3k_2^3k_3^3}\left[\left(\Pi^{\mathbf{k_1}}_{m_1n_1,ij}\Pi^{\mathbf{k_2}}_{m_2n_2,im}\Pi^{\mathbf{k_3}}_{m_3n_3,lj}-\frac{1}{2}\Pi^{\mathbf{k_1}}_{m_1n_1,ij}\Pi^{\mathbf{k_2}}_{m_2n_2,ml}\Pi^{\mathbf{k_3}}_{m_3n_3,ij}\right)k_{1m}k_{1l}+\text{ five permutations}\right]$$
$$\times\left[-k_T+\frac{k_1k_2+k_2k_3+k_3k_1}{k_T}+\frac{k_1k_2k_3}{k_T^2}\right].$$

Chapter 3

Numerical results

I shall now discuss the numerical methods used to evaluate the scalar field, the tensor power spectrum and the tensor bi-spectrum during two models of inflation, namely power law inflation and inflation driven by a quadratic potential model. The chapter is split into three sections on the inflation, on the tensor power spectrum and the tensor bi-spectrum. In each section, I shall discuss the numerical results for power law inflation and for inflation driven by a quadratic potential model. Also, as the tensor bi-spectrum is evaluated in three limits, namely in the equilateral limit, in the squeezed limit and for an arbitrary configuration of wavevectors, the section on tensor bi-spectrum is divided as such, in which the numerical results for power law inflation and for inflation driven by quadratic potential model will be discussed.

3.1 Numerical evaluation of the inflaton

As mentioned earlier, the scalar field driving the inflation is often referred to as the 'Inflation'. We assume that the potential $V(\phi)$ driving power law inflation is related to the scalar field ϕ as

$$V(\phi) = V_0 \exp\left[-\sqrt{\frac{2}{q}}\,(\phi - \phi_i)\right], \tag{3.1}$$

where ϕ_i is the value of the scalar field at $N = 0$ and q is the power law index. Recall that the equation governing the scalar field is given by

$$\ddot{\phi} + 3H\dot{\phi} + V_\phi = 0, \tag{3.2}$$

where $V_\phi = \mathrm{d}V/\mathrm{d}\phi$. We shall now rewrite the above equation in terms of e-fold N as

$$\frac{\mathrm{d}^2\phi}{\mathrm{d}N^2} + \left[3 - \frac{1}{2}\left(\frac{\mathrm{d}\phi}{\mathrm{d}N}\right)^2\right]\frac{\mathrm{d}\phi}{\mathrm{d}N} + \left[6 - \left(\frac{\mathrm{d}\phi}{\mathrm{d}N}\right)^2\right]\frac{1}{2V(\phi)}\frac{\mathrm{d}V(\phi)}{\mathrm{d}N} = 0. \tag{3.3}$$

Note that the the Hubble parameter H in the above equation is defined as

$$H^2 = \frac{2V(\phi)}{3 - (\mathrm{d}\phi/\mathrm{d}N)^2}. \tag{3.4}$$

We numerically solve the Eqn. (3.10) using an implementation of the fourth order Runge-Kutta method in Python [21, 22, 23]. Integration is performed from e-fold $N = 0$ to $N = 70$. Note that the initial conditions for solving the differential equation are

$$\phi = 1, \tag{3.5}$$

$$\frac{\mathrm{d}\phi}{\mathrm{d}N} = \left(\frac{\sqrt{2q}}{t_0}\frac{1}{H_0}\right), \tag{3.6}$$

where H_0 is the value of the Hubble parameter at $N = 0$. Also note that ϕ at $N = 0$ was referred to as ϕ_i in Eqn.(3.1). Figures 3.1 and 3.2 show the numerical estimates of the scalar field ϕ and the Hubble parameter H as a function of e-fold time N.

Similarly, the potential driving inflation in the quadratic potential model is

$$V(\phi) = \frac{1}{2}m^2\phi^2, \tag{3.7}$$

where $m = 7147 \times 10^{-9}$.

We arrive at a numerical solution for the scalar field during inflation driven by quadratic potential model in the same manner with which we arrived at the numerical results in the previous case, during power law inflation. We numerically solved the Eqn. (3.3) using a Runge-Kutta 4 method implemented in python. To arrive at the numerical solution, we assumed that the initial values for the scalar field, phi, and it's derivative with respect to e-fold N, $\mathrm{d}\phi/\mathrm{d}N$ as

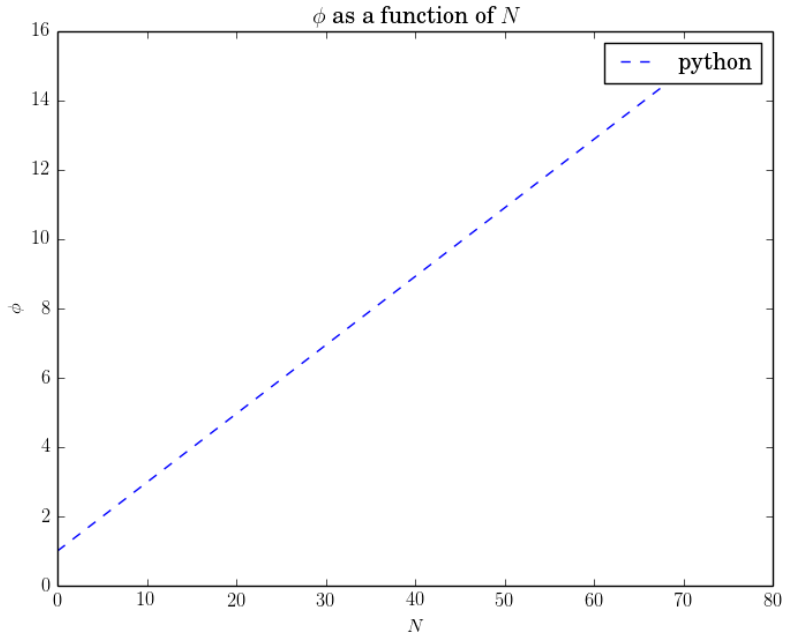

Figure 3.1: Numerical estimate of the scalar field ϕ as a function of N in power law inflation.

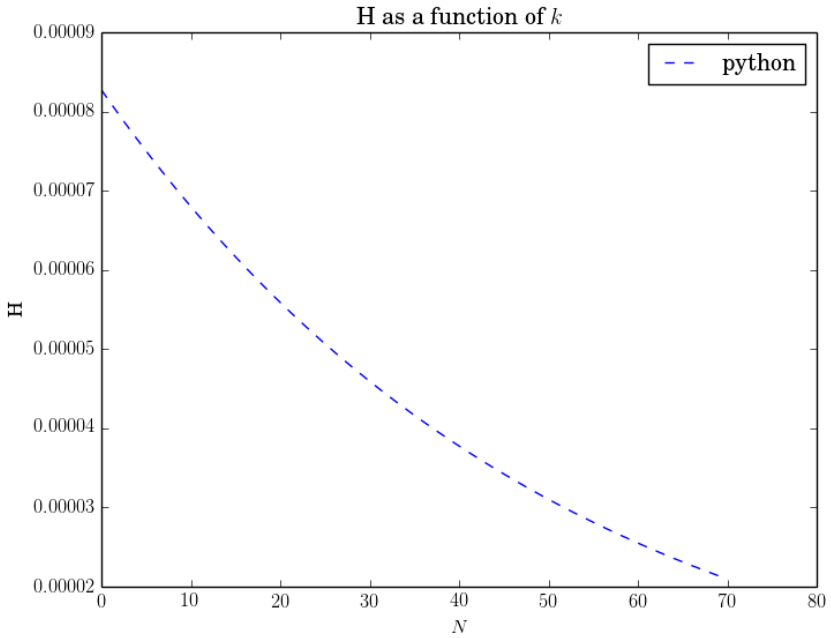

Figure 3.2: Numerical estimate of the Hubble parameter H as a function of N in power law inflation.

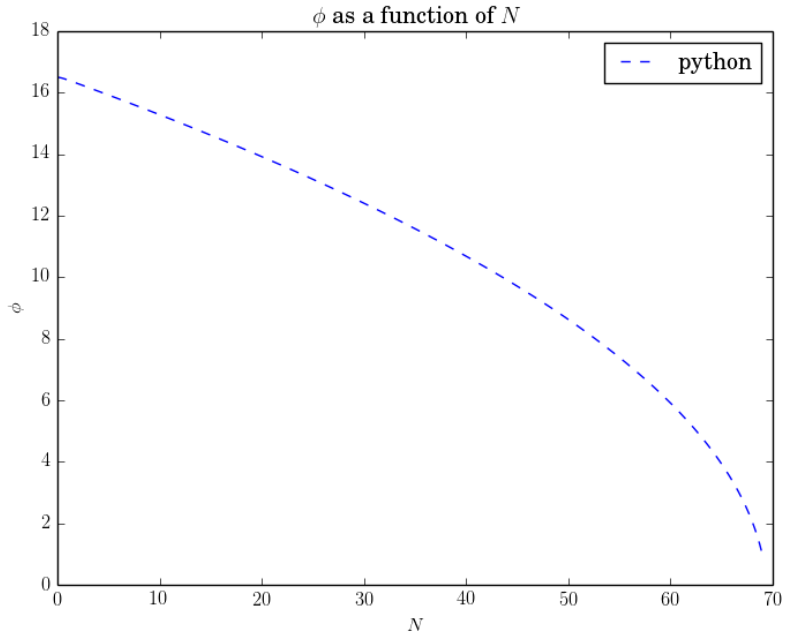

Figure 3.3: Numerical estimate of the scalar field ϕ as a function of N in inflation driven by quadratic potential model.

$$\phi = \frac{165}{10}, \tag{3.8}$$

$$\frac{\mathrm{d}\phi}{\mathrm{d}N} = -10^{-5}. \tag{3.9}$$

Figure 3.3 shows the numerical estimate of the scalar field with respect to e-fold N and Figure 3.4 shows the numerical estimate of the Hubble parameter, H, with respect to e-fold N during inflation driven by a quadratic potential model.

3.2 Numerical evaluation of the tensor power spectrum

The Eqn. (1.5) governing the evolution of tensor perturbations in cosmic time t can be rewritten in terms of e-fold N as

$$\frac{\mathrm{d}^2 h_k}{\mathrm{d}N^2} + \left(3 + \frac{1}{H}\frac{\mathrm{d}H}{\mathrm{d}N}\right)\frac{\mathrm{d}h_k}{\mathrm{d}N} + \frac{k^2}{a^2H^2}h_k = 0. \tag{3.10}$$

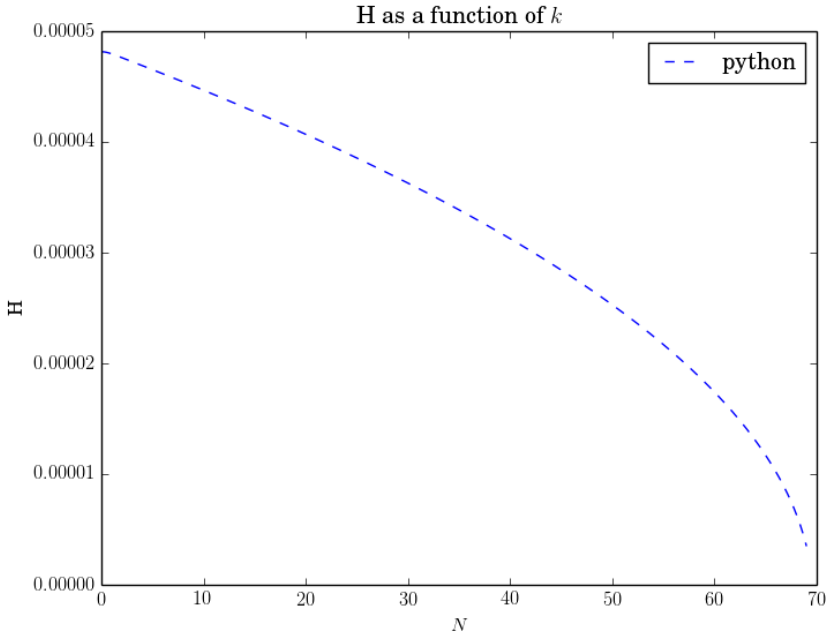

Figure 3.4: Numerical estimate of the Hubble parameter H as a function of N in inflation driven by quadratic potential model.

We can now solve the above second order differential equation numerically as we already have the numerical solution of the scalar field, ϕ, and Hubble parameter, H, as functions of e-fold N. Similar to the integration routine used to numerically estimate the scalar field ϕ, we use a fourth order Runge-Kutta method to solve the above equation numerically.

To arrive at the initial conditions to perform the numerical integration, we first need to arrive at an appropriate e-fold N. In our results, we choose to set the initial conditions when the modes are well inside the Hubble scale corresponding to the mode i.e $k/aH = 100$. We perform the numerical integration till e-fold N when the modes are well outside the Hubble radius i.e $k/aH = 10^{-5}$. Using the Bunch-Davies initial conditions, Eqn. (1.12), we can write h_k and $\mathrm{d}h_k/\mathrm{d}N$ in terms of e-fold N as

$$h_k = \frac{1}{\sqrt{2k_0}a(N)}, \tag{3.11}$$

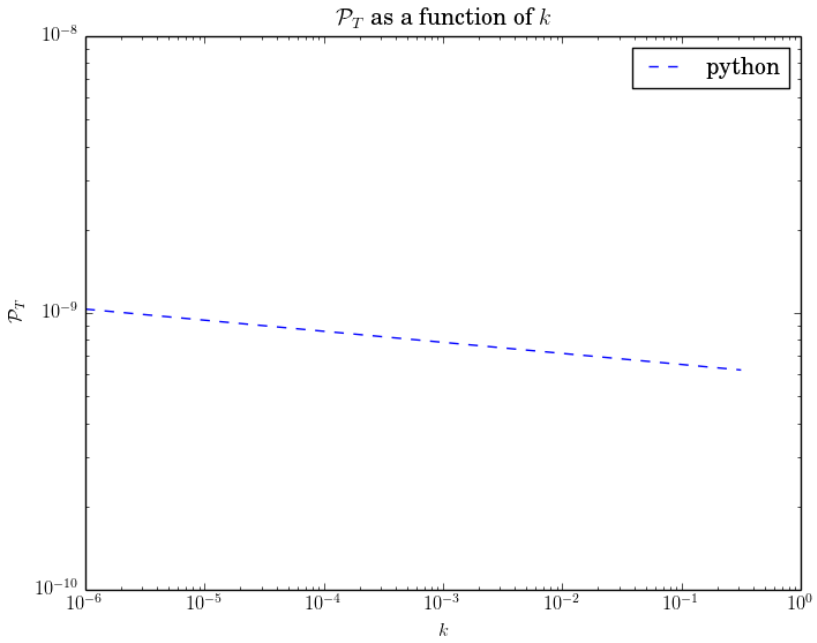

Figure 3.5: Numerical estimate of the tensor power spectrum $\mathcal{P}_{\rm T}$ as a function of k in power law inflation.

$$\frac{\mathrm{d}h_k}{\mathrm{d}N} = -\frac{1}{\sqrt{2k_0}a(N)} - \frac{i\sqrt{(k_0/2)}}{a^2(N)H(N)}, \tag{3.12}$$

From the numerical solution to h_k, we can evaluate the tensor power spectrum using Eqn. (1.11). Figure 3.5 shows the numerical solution of the tensor power spectrum $\mathcal{P}_T(k)$ during power law inflation as a function of k.

Similar to what we had done earlier, having arrived at the numerical solution for the background, we can now solve the Eqn. (3.10) that governs the evolution of the tensor perturbations during inflation to arrive at a numerical solution for the evolution of the tensor perturbations. Again, as mentioned earlier in the case for power law inflation, we assume that the initial conditions for tensor perturbations, h_k, and the derivative of the tensor perturbations with respect to e-fold N, $\mathrm{d}h_k/\mathrm{d}N$, using the Eqns. (3.11) and (3.12).

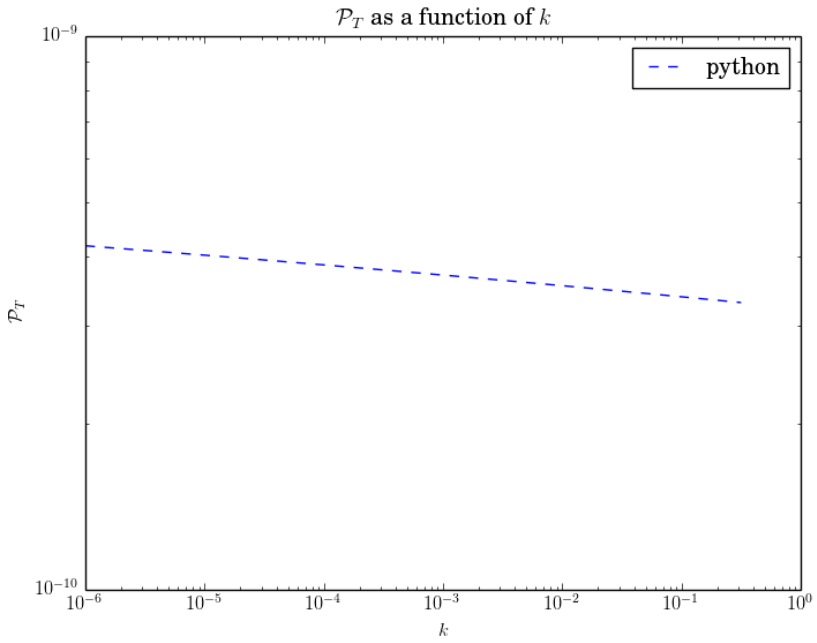

Figure 3.6: Numerical estimate of the tensor power spectrum $\mathcal{P}_{\rm T}$ as a function of k in inflation driven by quadratic potential model.

Figure 3.6 shows a numerical solution for the power spectrum of tensor perturbations in the super-Hubble limit during inflation driven by a quadratic potential model.

3.3 Numerical evaluation of the tensor bi-spectrum

As mentioned earlier, we neglect the polarization of the tensor perturbations. We can therefore rewrite the equation that defines tensor bi-spectrum, $G_{\gamma\gamma\gamma}$, and the non-Gaussianity parameter h_{NL} as

$$G_{\gamma\gamma\gamma} = h_{k_1}(\eta_e)h_{k_2}(\eta_e)h_{k_3}(\eta_e)\mathcal{G} + h^*_{k_1}(\eta_e)h^*_{k_2}(\eta_e)h^*_{k_3}(\eta_e)\mathcal{G}^*, \tag{3.13}$$

$$h_{NL} = \frac{k_1^3 k_2^3 k_3^3 G_{\gamma\gamma\gamma}}{k_1^3\mathcal{P}_T(\eta_e)\mathcal{P}_T(\eta_e) + k_2^3\mathcal{P}_T(\eta_e)\mathcal{P}_T(\eta_e) + k_3^3\mathcal{P}_T(\eta_e)\mathcal{P}_T(\eta_e)}, \tag{3.14}$$

where

$$\mathcal{G} = \frac{-i}{4}(k_1^2 + k_2^2 + k_3^2) \int_{\eta_i}^{\eta_e} \mathrm{d}\eta a(\eta) h_{k_1}^*(\eta) h_{k_2}^*(\eta) h_{k_3}^*(\eta). \tag{3.15}$$

While the equations governing the tensor bi-spectrum, $G_{\gamma\gamma\gamma}$, and the non-Gaussianity parameter, h_{NL}, can be trivially converted from cosmic time t to e-fold N, the integral $\mathcal{G}$ can be rewritten as

$$\mathcal{G} = \frac{-i}{4}(k_1^2 + k_2^2 + k_3^2) \int_{N_i}^{N_f} \mathrm{d}N \frac{a(N)}{H(N)} h_{k_1}^*(N) h_{k_2}^*(N) h_{k_3}^*(N). \tag{3.16}$$

It is to be noted that the function, h_k, and therefore the integral itself oscillate highly in the extreme sub-Hubble domain ($k\eta \to -\infty$). In order to regulate these integrals, we introduce a cut-off factor $e^{-\kappa k_T/3a(N)H(N)}$, where κ is a small positive quantity and k_T is the sum of the individual wavevectors. Such a cut-off also proves to be essential inorder to identify the correct perturbative vaccum.

3.3.1 Equilateral limit

In the equilateral limit, we assume that the three wavevectors, k_1, k_2 and k_3, have the same amplitude. We can therefore rewrite Eqn. (1.16) as

$$\mathcal{G} = \frac{-i}{4}(3k^2) \int_{N_i}^{N_f} \mathrm{d}N \frac{a(N)}{H(N)} h_k^*(N)^3 \tag{3.17}$$

We can solve the above integral as we already have the numerical solutions of the scale factor $a(N)$, the Hubble parameter $H(N)$ and the strength of tensor perturbations $h_k(N)$. We evaluate the integrals over the same limits in which we solved the Eqn. (3.10), i.e from when the modes are well inside the Hubble scale corresponding to the mode i.e $k/aH = 100$ till when the modes are well outside the Hubble radius i.e $k/aH = 10^{-5}$.

Figure 3.7 shows the dependence of $\mathcal{G}$ during power law inflation on the amplitude of the wavevector k.

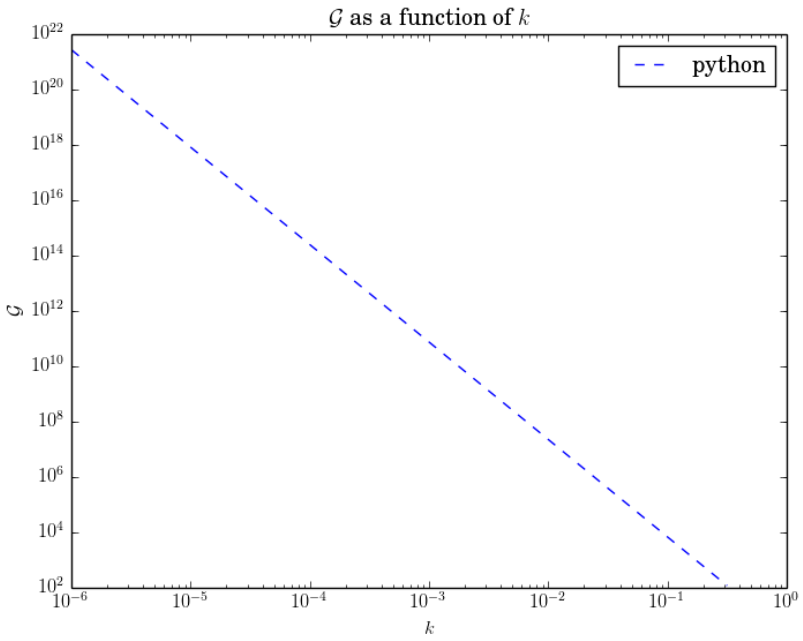

Figure 3.7: Numerical estimate of $\mathcal{G}$ as a function of k in the equilateral limit in power law inflation.

Figure 3.8 shows the numerical estimate of the tensor bi-spectrum $G_{\gamma\gamma\gamma}$ during power law inflation as a function of k. Given the dependence of h_k and $\mathcal{G}$ on k, we can arrive at the fact that $k^6 G_{\gamma\gamma\gamma}$ is an invariant quantity. The figure 3.9 shows the invariance of $k^6 G_{\gamma\gamma\gamma}$ as a function of k. The blue dotted line denotes the numerical results obtained where as the green crosses represents

$$k^6 G_{\gamma\gamma\gamma}(k) \propto k^{4(\gamma+2)}. \tag{3.18}$$

where the γ on the left hand side denote the tensor perturbations and the γ on the right hand side denotes the exponent in the Eqn. (2.10).

We can finally estimate the value of the non-Gaussianity parameter h_{NL} during power law inflation using Eqn. (3.14). Figure 3.10 shows the dependence of h_{NL} as a function of k. As you can see, the value of the h_{NL} is invariant in k.

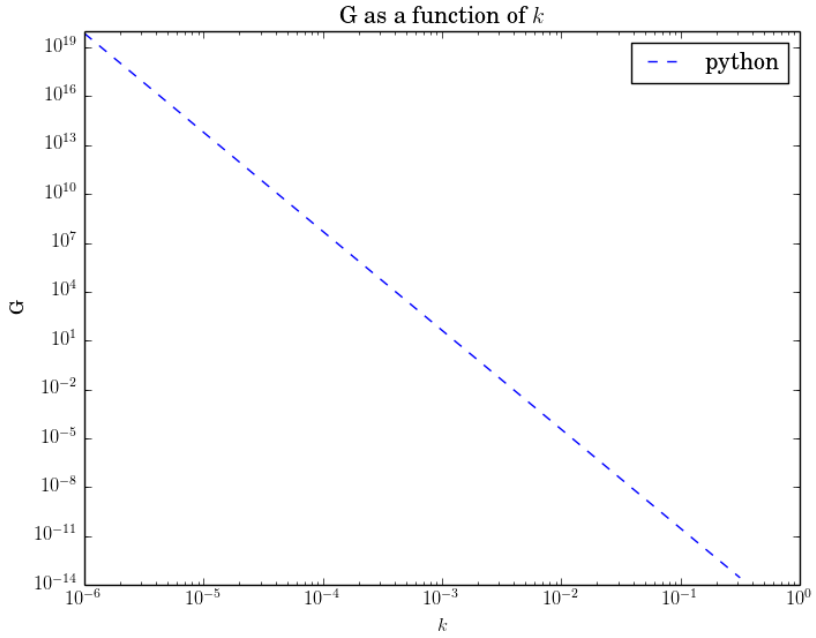

Figure 3.8: Numerical estimate of the tensor bi-spectrum $G_{\gamma\gamma\gamma}$ as a function of k in the equilateral limit in power law inflation.

Similar to the earlier case in power law inflation, having arrived at a numerical solution for the evolution of tensor perturbations during inflation driven by quadratic potential earlier, we can now evaluate the tensor bi-spectrum numerically. Again, as in the case with power law inflation earlier, we solve the Eqn. (3.17) numerically to arrive at the integral $\mathcal{G}$ using which we can arrive at the tensor bi-spectrum, $G_{\gamma\gamma\gamma}$, and the non-Gaussianity parameter, h_{NL}.

Figure 3.11 shows the numerical solution to the integral $\mathcal{G}$ with respect to e-fold wavenumber k. Figure 3.12 shows the numerical solution to the tensor bi-spectrum $G_{\gamma\gamma\gamma}$ as a function wavenumber k. Figure 3.13 shows the invariance of $k^6 G_{\gamma\gamma\gamma}$ with respect to k. Figure 3.14 shows the numerical solution of the non-Gaussianity parameter, h_{NL}, during inflation driven by quadratic potential model with respect to wavenumber k.

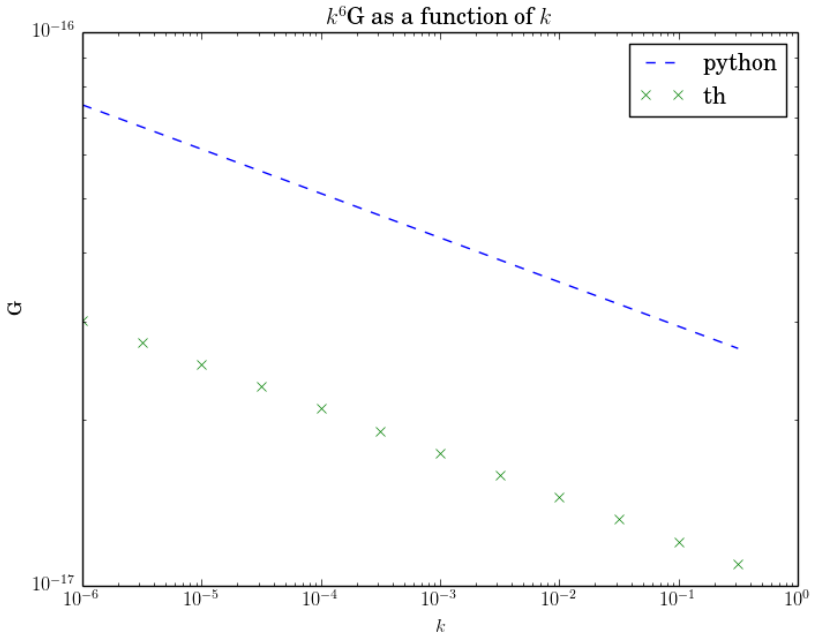

Figure 3.9: Numerical estimate of the invariant $k^6 G_{\gamma\gamma\gamma}$ as a function of k in the equilateral limit in power law inflation. The blue dashes represent the numerical results and the green crosses represent the theoretical form of the invariance. The green crosses are displayed to show the similarity in behaviour and not in the difference in results.

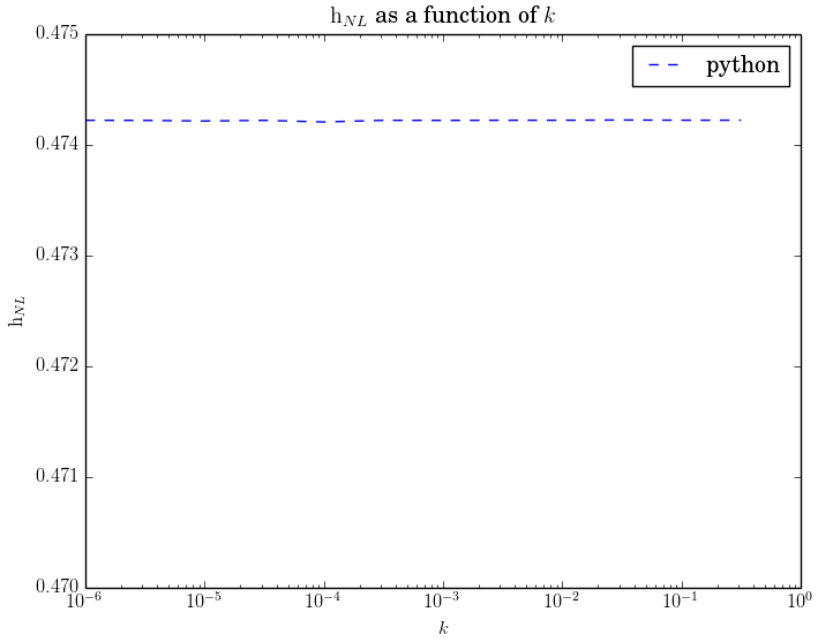

Figure 3.10: Numerical estimate of the non-Gaussianity parameter h_{NL} as a function of k in the equilateral limit in power law inflation.

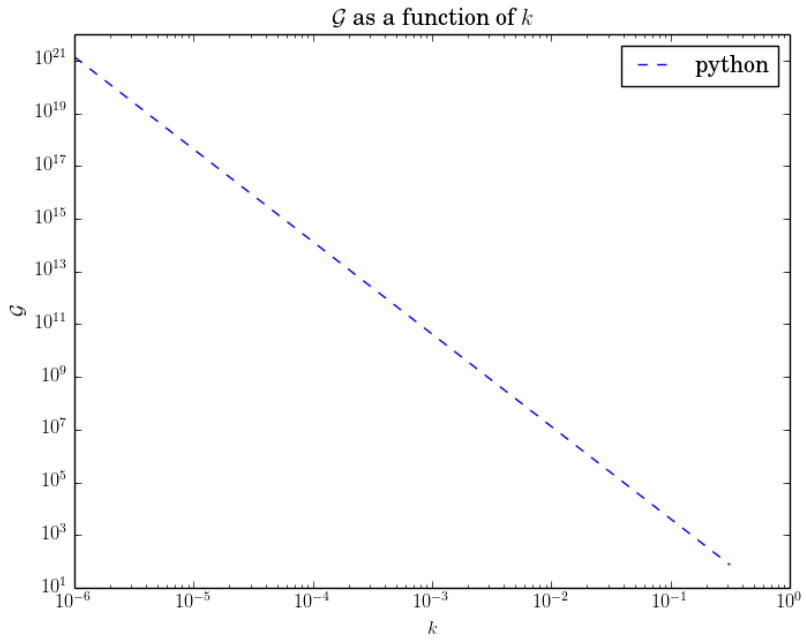

Figure 3.11: Numerical estimate of $\mathcal{G}$ as a function of k in the equilateral limit in inflation driven by quadratic potential model.

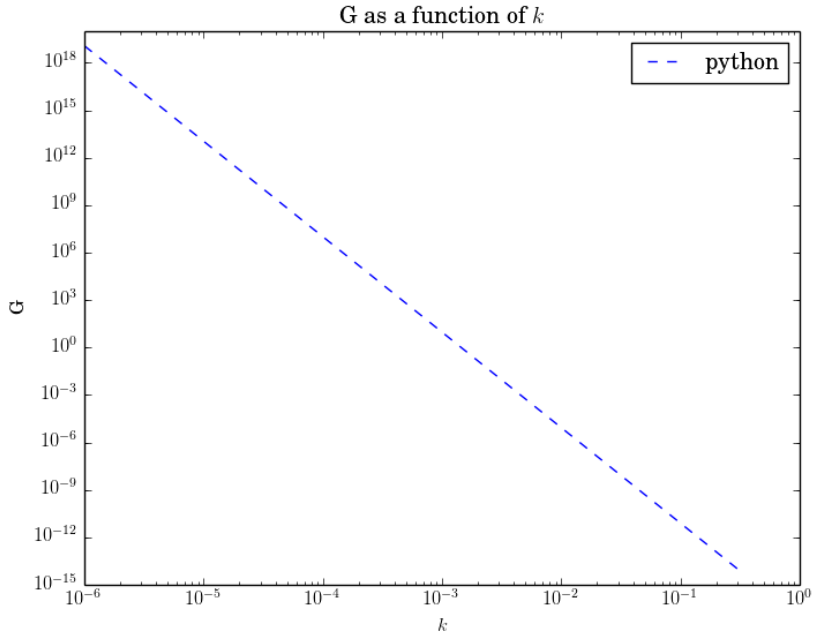

Figure 3.12: Numerical estimate of the tensor bi-spectrum $G_{\gamma\gamma\gamma}(k)$ as a function of k in the equilateral limit in inflation driven by quadratic potential model.

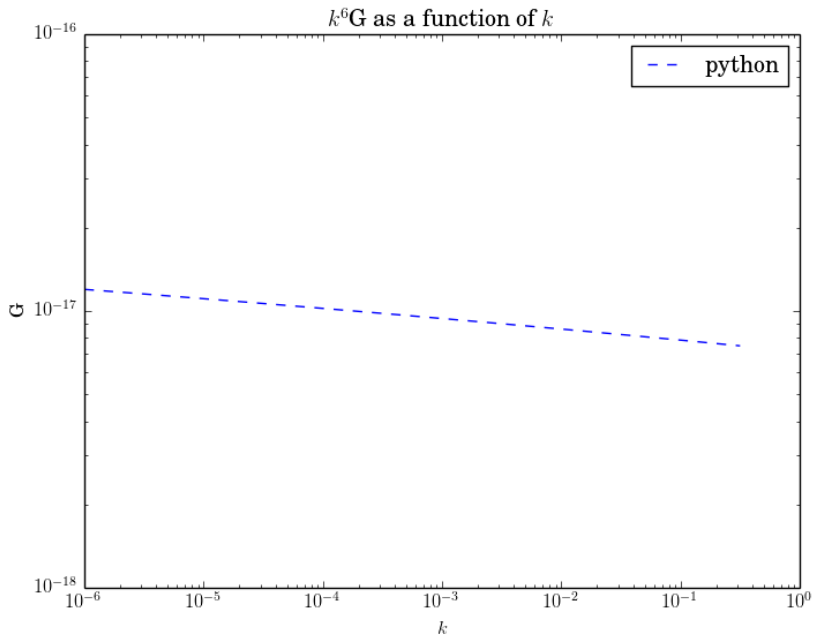

Figure 3.13: Numerical estimate of the invariant $k^6 G_{\gamma\gamma\gamma}(k)$ as a function of k in the equilateral limit in inflation driven by quadratic potential model.

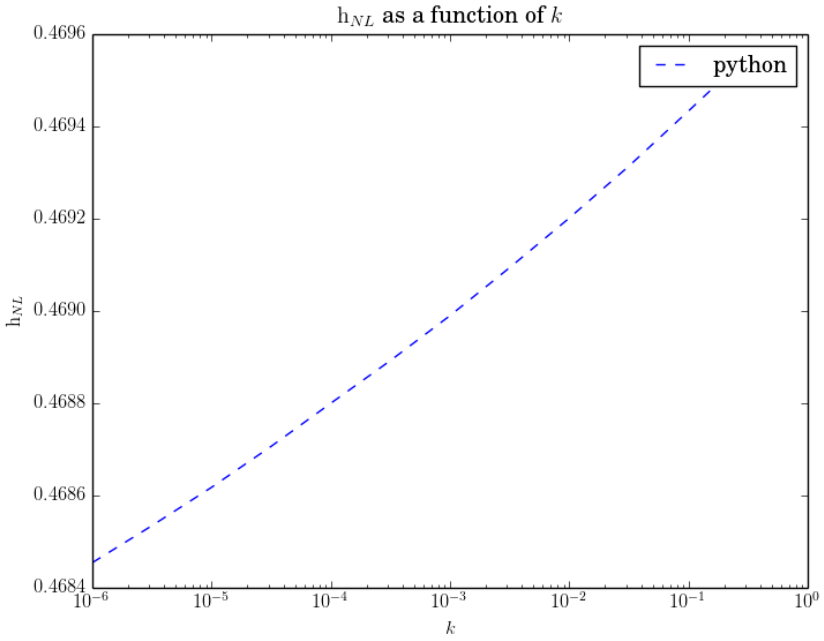

Figure 3.14: Numerical estimate of the non-Gaussianity parameter h_{NL} as a function of k in the equilateral limit in inflation driven by quadratic potential model.

3.3.2 Squeezed limit

In the squeezed limit, we assume that the amplitude of two of the modes is equal, say $|k_1| = |k_2| = |k|$ and we assume k_3 to be a pseudo-zero mode, k_0, with an amplitude much smaller than k. We numerically arrive at the solutions of k and k_0 independently following which we evaluate the integral in $\mathcal{G}$ from η_i corresponding to the smallest mode, k_0, till η_e corresponding to the largest mode, k.

Figure 3.15 shows the numerical estimate of the tensor bi-spectrum value $G_{\gamma\gamma\gamma}$ during power law inflation as a function of k in the squeezed limit and figure 3.16 shows the invariance of $k^{3/2}k_0^{3/2}G_{\gamma\gamma\gamma}$, where the blue dashed line denotes the numerical results where as the green crosses represent

$$k_1^3 k^3 G_{\gamma\gamma\gamma}^{m_1 n_1 m_2 n_2 m_3 n_3}(k_1, k) \propto k_1^{2(\gamma+2)} k^{2(\gamma+2)}, \tag{3.19}$$

where the γ on the left hand side denote the tensor perturbations and the γ on the right hand

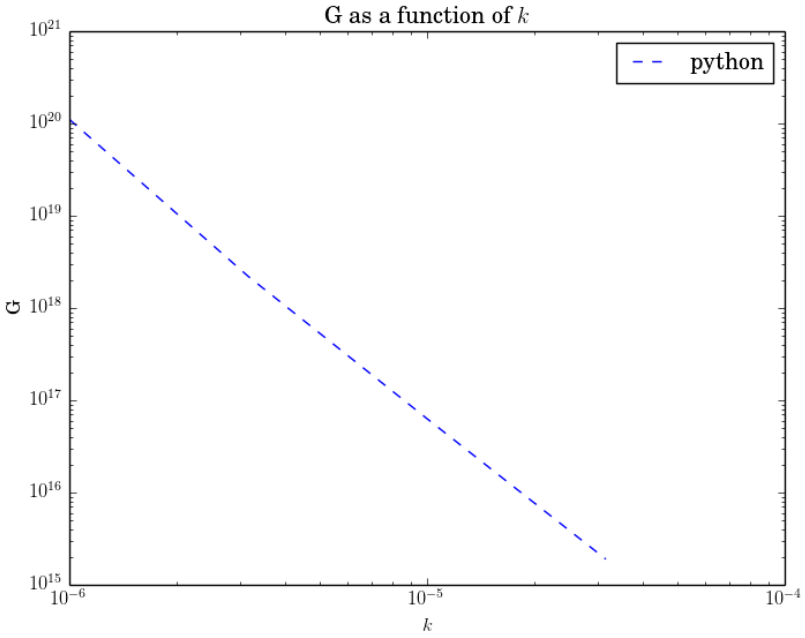

Figure 3.15: Numerical estimate of the tensor bi-spectrum $G_{\gamma\gamma\gamma}$ as a function of k in the squeezed limit in power law inflation.

side denotes the exponent in the Eqn. (2.10) and k_1 denotes the pseudo-zero wavevector in the squeezed limit.

Figure 3.17 shows the numerical estimate of the non-Gaussianity parameter h_{NL} during power law inflation as a function of k in the squeezed limit and as you can see, h_{NL} reaches an invariant value.

Similar to the previous case for power law inflation, when we estimated the tensor bi-spectrum in the squeezed limit during power law inflation, we set $|k_1| = |k_2| = |k|$ and we $|k_3| = |k_0|$, where $|k| \gg |k_0|$. Using the above assumption and the numerical solutions to the tensor perturbations for various k, we first arrive at a numerical estimate of the integral, $\mathcal{G}$, using which we can estimate the tensor bi-spectrum, $G_{\gamma\gamma\gamma}$, and the non-Gaussianity parameter, h_{NL}, as a function of wavenumber k.

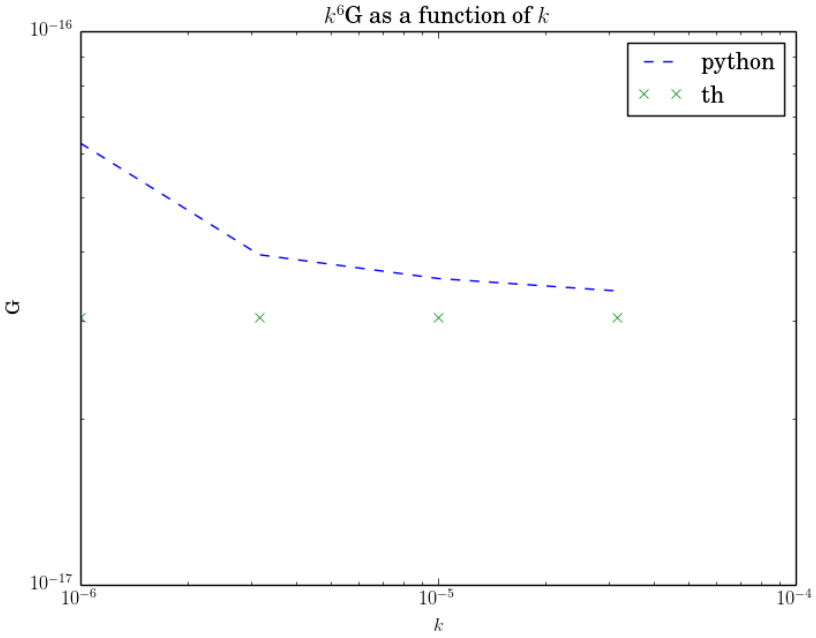

Figure 3.16: Numerical estimate of the invariant $k_0^{3/2}k^{3/2}G_{\gamma\gamma\gamma}(k)$ as a function of k in the squeezed limit in power law inflation. The blue dashes represent the numerical results and the green crosses represent the theoretical form of the invariance. The green crosses are displayed to show the similarity in behaviour and not in the difference in results.

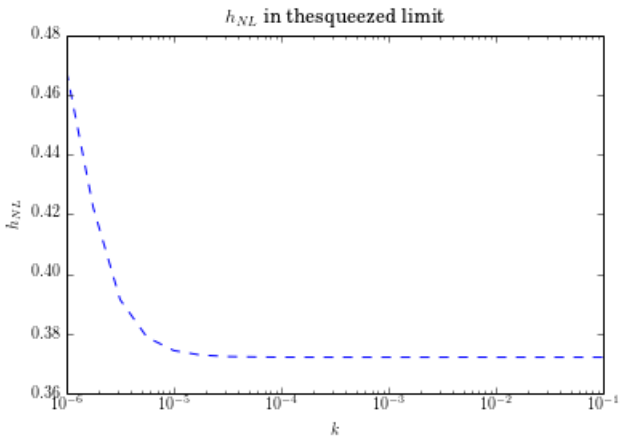

Figure 3.17: Numerical estimate of the non-Gaussianity parameter h_{NL} as a function of k in the squeezed limit in power law inflation.

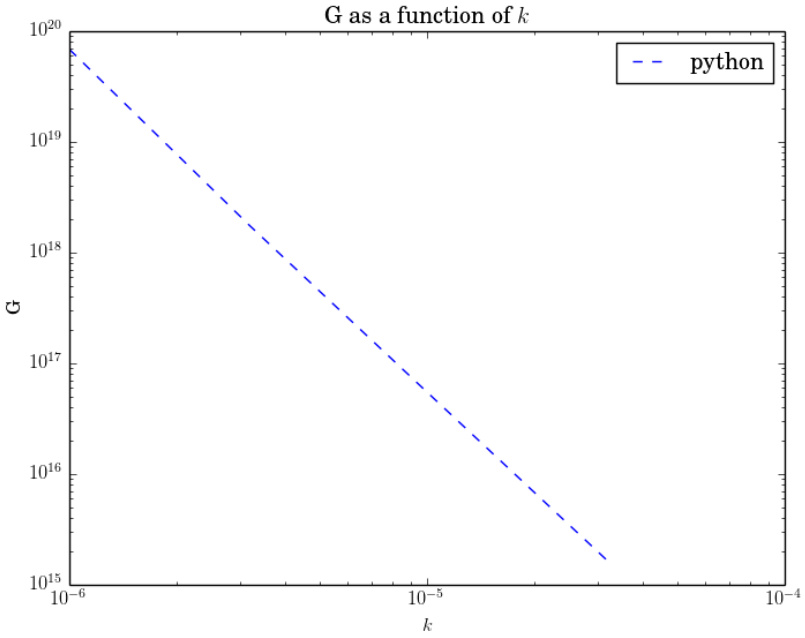

Figure 3.18: Numerical estimate of the tensor bi-spectrum $G_{\gamma\gamma\gamma}(k)$ as a function of k in the squeezed limit in inflation driven by quadratic potential model.

Figure 3.18 shows the numerical estimate of the tensor bi-spectrum during inflation driven by a quadratic potential model and Figure 3.19 shows the invariance of $k^3 k_0^3 G_{\gamma\gamma\gamma}$ with respect to the wavenumber k in the squeezed limit. Figure 3.20 shows the numerical estimate of the non-Gaussianity parameter, h_{NL}, with respect to k.

3.3.3 Triangular configuration of wavevectors

In this case, we consider wavevectors, $\mathbf{k}_1, \mathbf{k}_2$ and $\mathbf{k}_3$ which form a triangle. Numerically speaking, we fix $|k_1| = 1e-02$ and we vary $|k3|$ from 0 till $1e-02$. From these two values and the fact that

$$|k_1|^2 + |k_2|^2 + |k_3|^2 = 1, \tag{3.20}$$

we can estimate the value of $|k2|$. We solve the Eqn. (3.10) to find the numerical solutions to this triangular configuration of wavevectors. Numerically, we solve the Eqn. (3.10) from N_i corresponding to the smallest wavevector a till N_f corresponding to the largest wavevector

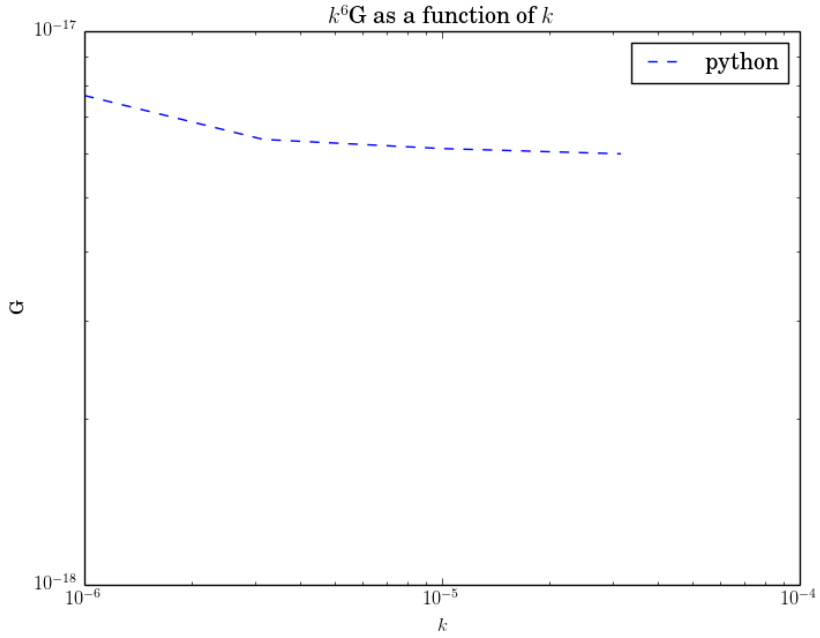

Figure 3.19: Numerical estimate of the invariant $k_0^{3/2}k^{3/2}G_{\gamma\gamma\gamma}(k)$ as a function of k in the squeezed limit in inflation driven by quadratic potential model.

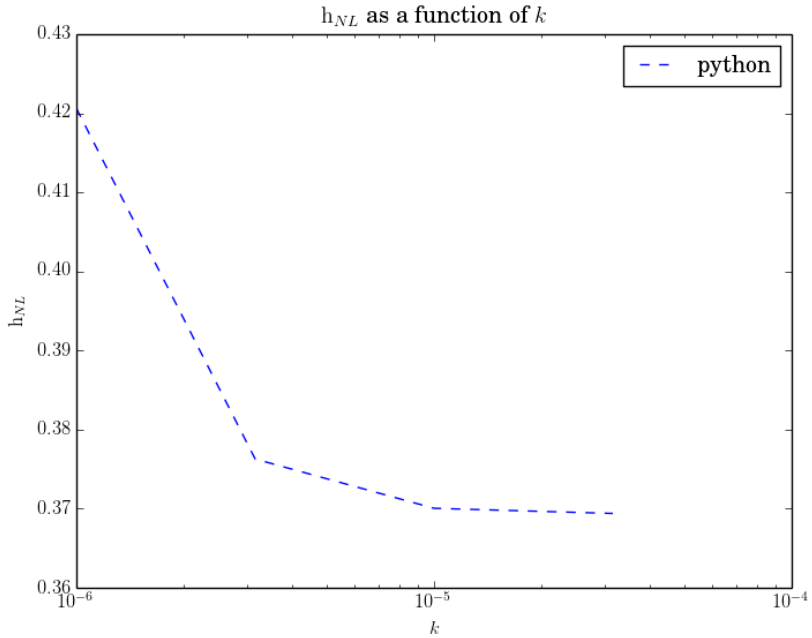

Figure 3.20: Numerical estimate of the non-Gaussianity parameter h_{NL} as a function of k in the squeezed limit in inflation driven by quadratic potential model.

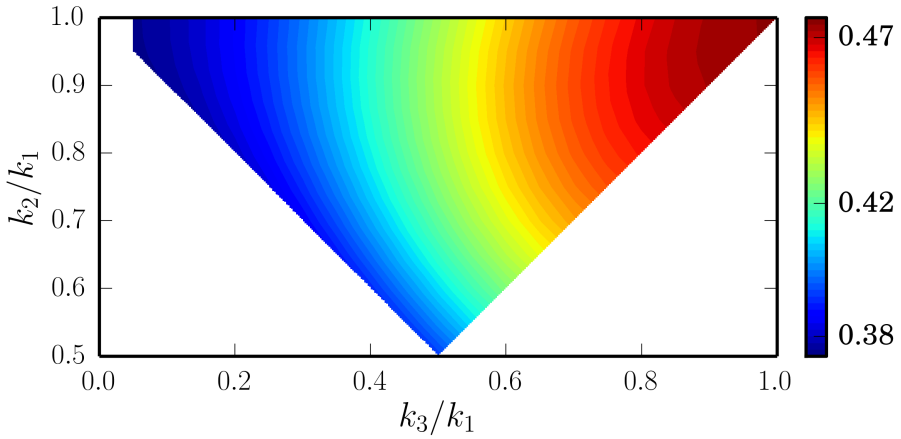

Figure 3.21: Density plot of the numerical estimates of the non-Gaussianity parameter h_{NL} as a function of k for a triangular configuration of wavevectors in power law inflation. The left hand corner of the triangle plot is chipped off because of the fact that we cannot numerically approach $k = 0$.

where N_i and N_f are e-fold N when the modes are well inside the Hubble scale corresponding to the mode i.e $k/aH = 100$ and when the modes are well outside the Hubble radius i.e $k/aH = 10^{-5}$.

Figure 3.21 shows the h_{NL} values during power law inflation for such a triangular configuration of wavevectors.

Similar to the numerical procedure carried out in the earlier case, in power law inflation, we evaluate h_{NL} for wavevectors $\mathbf{k}_1, \mathbf{k}_2, \mathbf{k}_3$ which form a triangular configuration. As mentioned previously, we set $|k_1| = 10^{-2}$ and we obtain the corresponding values of $|k_2|$ and $|k_3|$.

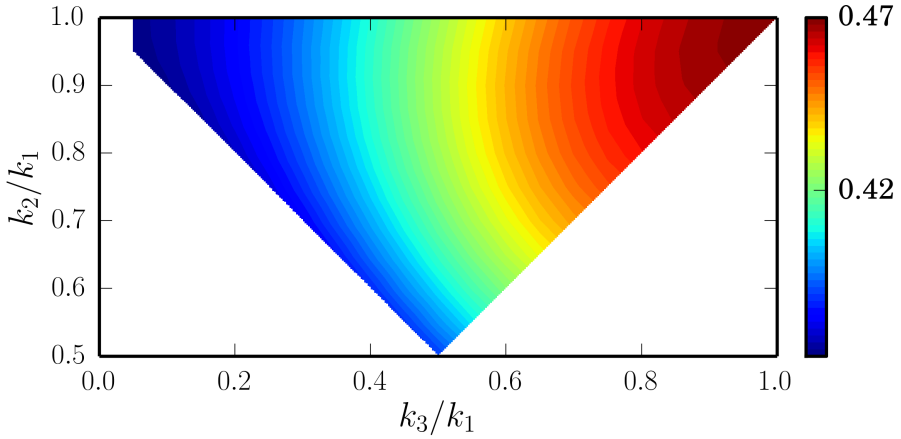

Figure 3.22: Density plot of the non-Gaussianity parameter h_{NL} as a function of k for a triangular configuration of wavevectors in inflation driven by quadratic potential model.The left hand corner of the triangle plot is chipped off because of the fact that we cannot numerically approach $k = 0$.

Fig 3.22 represents numerical estimates of non-Gaussianity parameter, h_{NL} , during inflation driven by a quadratic potential model for a triangular configuration of wavevectors.

Chapter 4

Summary

In this work, we have studied the tensor perturbations in the metric and evaluated the power spectrum and bi-spectrum of tensor perturbations. We then looked at analytic solutions to the tensor power spectrum and the tensor bi-spectrum during power law inflation and during slow roll inflation. We have also numerically evaluated the tensor bi-spectrum in the super-Hubble limit in power law inflation and for inflation driven by a quadratic potential model.

In the first chapter, we discussed the theory of inflation briefly and the constraints on a scalar field driving inflation. By studying the stress-energy tensor corresponding to the scalar field, we were able to arrive at the equation governing the evolution of the scalar field. Having solved for the background, we studied the perturbed Einstein tensors and the perturbed stress-energy tensor to arrive at the equation governing the evolution of the tensor perturbations. We then quantized the tensor perturbations and arrived at an analytic form of the power spectrum of tensor perturbations. We then defined the tensor bi-spectrum, $G_{\gamma\gamma\gamma}$, using the Maldacena formalism and the non-Gaussianity parameter, h_{NL}.

In the second chapter, we discussed the analytical solutions to the tensor perturbations in two models of inflation, namely power law inflation and slow roll inflation. We discussed the analytical solutions to the scalar field phi in both of the cases and using the solutions to the background, we arrived at the analytical expressions to the evolution of the tensor perturbations with respect to conformal time, η. We then attempted to arrive at an analytic expression for the tensor bi-spectrum $G_{\gamma\gamma\gamma}$ in slow roll inflation.

In the third chapter, we discussed the numerical methods implemented to solve the background equations and the equations governing tensor perturbations in two models of inflation, namely power law inflation and inflation driven by a quadratic potential model. Having solved for the tensor perturbations, we evaluate the relevant integrals and estimate the tensor bi-spectrum, $G_{\gamma\gamma\gamma}$, and the non-Gaussianity parameter, h_{NL}, in the super-Hubble limit. We evaluated the tensor bi-spectrum, $G_{\gamma\gamma\gamma}$, and the non-Gaussianity parameter, h_{NL}, numerically in the equilateral limit, in the squeezed limit and for a triangular configuration of wavevectors.

Bibliography

[1] J. Dunkley et al., Astrophys. J. Suppl. 180, 306 (2009); E. Komatsu et al., Astrophys. J. Suppl. 180, 330 (2009).

[2] P. A. R. Ade et al., arXiv:1303.5075 [astro-ph.CO].

[3] L. Sriramkumar, arXiv:0904.4584.

[4] S. Dodelson, Modern Cosmology (Academic Press, San Diego, 2003).

[5] R. Durrer, Fund. Cosmic Phys. **15**, 209 (1994).

[6] A. Riotto, arXiv:hep-ph/0210162.

[7] W. H. Kinney, astro-ph/0301448.

[8] A. D. Linde, Particle Physics and Inflationary Cosmology (Harwood Academic, Switzerland, 1990).

[9] R. H. Brandenberger, Rev. Mod. Phys. **1**, 57 (1985).

[10] V. F. Mukhanov, H. A. Feldman, and R. H. Brandenberger, Phys. Rep. **215**, 203 (1992).

[11] M. Giovannini, Int. J. Mod. Phys. D **14**, 363 (2005).

[12] A. Guth, Phys. Rev. D **23**, 347 (1981).

[13] M. Abramowitz and I. A. Stegun, Handbook of Mathematical Functions (Dover Publications, New York, 1964).

[14] NIST Digital Library of Mathematical Functions. http://dlmf.nist.gov/, Release 1.0.10 of 2015-08-07. Online companion to [OLBC10].

[15] J. Maldacena, JHEP 0305, 013 (2003).

[16] D. Jeong and M. Kamionkowski, Phys. Rev. Lett. 108, 251301 (2012); L. Dai, D. Jeong and M. Kamionkowski, Phys. Rev. D 87, 103006 (2013); Phys. Rev. D 88, 043507 (2013).

[17] S. Kundu, arXiv:1311.1575 [astro-ph.CO].

[18] X. Gao, T. Kobayashi, M. Shiraishi, M. Yamaguchi, J. Yokoyama and S. Yokoyama, arXiv:1207.0588 [astro-ph.CO].

[19] J. Maldacena and G. L. Pimentel, JHEP 1109, 045 (2011); X. Gao, T. Kobayashi, M. Yamaguchi and J. Yokoyama, Phys. Rev. Lett. 107, 211301 (2011).

[20] V. Sreenath, R. Tibrewala and L. Sriramkumar, JCAP 1312, 037 (2013).

[21] Guido van Rossum: Python Reference Manual, CWI Report CS-R9525 (1995).

[22] Stefan van der Walt, S. Chris Colbert and Gael Varoquaux, Computing in Science and Engineering **13**, 22 (2011).

[23] John D. Hunter, Computing in Science and Engineering **9**, 90 (2007).

Appendix A

Python code : Arbitrary triangular configuration of wavevectors

As previously mentioned, all of the numerical work was carried out using Python and the following is the Python code used to estimate the non-Gaussianity parameter, $h_{\rm NL}$, for a triangular configuration of wavevectors in power law inflation

We first solve the background to arrive at how the Hubble parameter, H, and it's first derivative, $\mathrm{d}H/\mathrm{d}N$, evolve during power law inflation. Using H and $\mathrm{d}H/\mathrm{d}N$, we numerically arrive at the evolution of the tensor perturbations. We then arrive at $\mathcal{G}$, the tensor bi-spectrum, $G_{\gamma\gamma\gamma}$, and finally the non-Gaussianity parameter, h_{NL}.

```
import numpy
from scipy.integrate import simps

import time
import multiprocessing as mp
import random
import string

parallel_output = mp.Queue()

q = 51.
V0 = (204./100.)*1e-08
t0 = (q*(3.*q -1.)/V0)**(1./2)

phi0 = 1.
dphi0 = (2.*q)**(1./2)/t0
```

```
Ni = 0.
Nf = 70.

# Note that in this code, I use the prefix 'd' to represent
derivative with respect to time (except for the case of dV
where the derivative is with respect to phi) and the prefix 'D'
to represent derivative with respect to e-fold N. Also, the
suffix '0' is used to represent the initial conditions in various
cases. Also, as can be seen here, we evaluate the scalar field
in the e-fold N range Ni to Nf.

V = lambda _phi : V0*numpy.exp(-(2./q)**(1./2)*(_phi -phi0))
dV = lambda _phi : -(2./q)**(1./2)*V0
*numpy.exp(-(2./q)**(1./2)*(_phi -phi0))

''' Functions to evaluate the values of the potential function V(phi)
and the derivative of V with respect to phi.
Note that functions can be defined using the lambda notation, as shown
above or using the usual def and return statements, as shown below.'''

H0 = ((1./3)*(dphi0**(2.)/2. +V(phi0)))**(1./2.)
Dphi0 = dphi0/H0

def DDphi(_N, _phi, _Dphi):
    ''' Returns the value of the second derivative of
    phi with respect to e-fold N.'''
    return -(3. -_Dphi**(2.)/2.)*_Dphi -(dV(_phi)/
     (2.*V(_phi)))*(6. -_Dphi**(2.))

def phi_rk4_step(_N, _phi, _Dphi, _step):
    ''' Returns 2 values, the first of the two is the value by which phi
    needs to be updated and the second of the two is the value by which the
    first derivative of phi with respect to e-fold N needs to be updated.'''
    F1 = _Dphi
    f1 = DDphi(_N, _phi, _Dphi)
    F2 = _Dphi +f1*_step/2.
    f2 = DDphi(_N +_step/2., _phi +F1*_step/2., _Dphi +f1*_step/2.)
    F3 = _Dphi +f2*step/2.
    f3 = DDphi(_N +_step/2., _phi +F2*_step/2., _Dphi +f2*_step/2.)
    F4 = _Dphi +f3*step
    f4 = DDphi(_N +_step, _phi +F3*_step, _Dphi +f3*_step)

    return (F1 +2.*F2 +2.*F3 +F4)*_step/6., (f1 +2.*f2 +2.*f3 +f4)*_step/6.

'''We evolve the scalar field phi for e-fold N ranging from Ni to Nf.'''
```

```
npts = 100000
step = (Nf-Ni)/(npts)

phi_ = phi0
Dphi_ = Dphi0

phi_array = numpy.empty(0)
Dphi_array = numpy.empty(0)
N_array = numpy.empty(0)

N = Ni
while N < Nf +step:
    phi_array = numpy.append(phi_array, phi_)
    Dphi_array = numpy.append(Dphi_array, Dphi_)
    N_array = numpy.append(N_array, N)

    phi_update, Dphi_update = phi_rk4_step(N, phi_, Dphi_, step)
    phi_ = phi_ +phi_update
    Dphi_ = Dphi_ +Dphi_update

    N += step

#2000001
#2000000
N_new = numpy.linspace(Ni,Nf,2000001)
phi_array_new = numpy.interp(N_new, N_array, phi_array)
Dphi_array_new = numpy.interp(N_new, N_array, Dphi_array)

phi_array = phi_array_new
Dphi_array = Dphi_array_new
N_array = N_new
step = (Nf-Ni)/(2000000)

phi = lambda _N : phi_array[int((_N-Ni)/step)]
Dphi = lambda _N : Dphi_array[int((_N-Ni)/step)]

H = lambda _N : (V(phi(_N))/(3. -Dphi(_N)**(2.)/2.))**(1./2)
DH = lambda _N : -(1./2)*H(_N)*Dphi(_N)**2.

'''The above functions let us access the values of H(N) and DH(N)
when we try to evaluate the tensor perturbations h_k. We have obtained
these values from the phi and Dphi values earlier.'''

ai = 1e-05
A = lambda _N : ai*numpy.exp(_N)
'''The scale factor in terms of e-fold N.'''
```

```
def DDhk(_k, _N, _hk, _Dhk):
    '''Returns the value of the second derivative of the tensor
    perturbations h_k with respect to e-fold N. We need this
    value when we are trying to evaluate h_k'''
    return -((3. +(DH(_N)/H(_N)))*_Dhk +((_k/(A(_N)*H(_N)))**(2.))*_hk)


def hk_rk4_step(_k, _N, _hk, _Dhk, _step):
    '''a runge-kutta 4 stepper function that returns the value by which
    h_k nd Dh_k need to be updated.'''
    F1 = _Dhk
    f1 = DDhk(_k, _N, _hk, _Dhk)
    F2 = _Dhk +f1*_step/2.
    f2 = DDhk(_k, _N +_step/2., _hk +F1*_step/2., _Dhk +f1*_step/2.)
    F3 = _Dhk +f2*_step/2.
    f3 = DDhk(_k, _N +_step/2., _hk +F2*_step/2., _Dhk +f2*_step/2.)
    F4 = _Dhk +f3*_step
    f4 = DDhk(_k, _N +_step, _hk +F3*_step, _Dhk +f3*_step)

#    print f1, f2, f3, f4, F1, F2, F3, F4, _step

    return (f1 +2.*f2 +2.*f3 +f4)*_step/6., (F1 +2.*F2 +2.*F3 +F4)*_step/6.
           # [Dhk, hk] update

def solve_Nics(k, eN_array):
    '''Returns the value of e-fold N when the mode is
    in the sub-Hubble domain, which we define as k/(A*H) =10^2.'''
    Ni = eN_array[0]
    step = eN_array[1] -eN_array[0]
    Nics_temp = numpy.asarray([k - 1e+02*A(N)*H(N) for N in eN_array])
    nics_test = numpy.where(Nics_temp > 0)
    return Ni + nics_test[0][-1]*step

def solve_Nshss(k, eN_array):
    '''Returns the value of e-fold N when the mode is
    in the super-Hubble domain, which we define as k/(A*H) =10^(-5).'''
    Ni = eN_array[0]
    step = eN_array[1] -eN_array[0]
    Nshss_temp = numpy.asarray([k - 1e-05*A(N)*H(N) for N in eN_array])
    nshss_test = numpy.where(Nshss_temp > 0)
    return Ni + nshss_test[0][-1]*step

def initialize_hk(k, _Nics):
    '''Returns the value of h_k for the mode k at e-fold N of _Nics.
    We obtain his value by imposing the Bunch-Davies initial conditions'''
```

```
    hk0 = numpy.zeros(1,dtype=complex)
    hk0.real = (((k)**(1./2))*A(_Nics))**(-1.)
    return hk0

def initialize_Dhk(k, _Nics):
    '''Returns the value of h_k for the mode k at e-fold N of _Nshss.
    We obtain his value by imposing the Bunch-Davies initial conditions'''
    Dhk0 = numpy.zeros(1,dtype=complex)
    Dhk0.real = -(1./A(_Nics))*((k)**(-1./2))
    Dhk0.imag = -((k)**(1./2))/(A(_Nics)*A(_Nics)*H(_Nics))
    return Dhk0

def evolve_hk(k, _Nics, _Nshss, _step):
    '''Returns the values of h_k for the mode k for e-fold N ranging from
    _Nics to _Nshss. We use the h_k values later on to estimate calG.'''
    hk = numpy.empty(0, dtype=complex)
    Dhk = numpy.empty(0, dtype=complex)

    hk = initialize_hk(k, _Nics)
    Dhk = initialize_Dhk(k, _Nics)

    hk_array = numpy.empty(0, dtype=complex)

    N = _Nics
    while N < _Nshss:
        hk_array = numpy.append(hk_array, hk)

        array = hk_rk4_step(k, N, hk, Dhk, _step)
        hk = hk + array[1]
        Dhk = Dhk + array[0]

        N += _step

    return hk_array

def calG(hk_k1_array, hk_k2_array, hk_k3_array,
k1, k2, k3, _Nics, _Nshss):
    '''Returns the value of \mathcal{G} which is in turn used to
    estimate G, the tensor bi-spectrum. The integral is evaluated
    for e-fold N ranging from _Nics till _Nshss. Note that the extra
    factor exp(-(e*k)/(A*H)) is put in by hand to satisfy the
    consistency relation.'''
    N_range = numpy.linspace(_Nics, _Nshss, len(hk_k1_array))
    func_int = ((A(N_range)/numpy.asarray([H(N) for N in N_range]))*
                (numpy.conj(hk_k1_array)*numpy.conj(hk_k2_array)
                *numpy.conj(hk_k3_array))*
```

```
                (numpy.exp(-e*(k1 +k2 +k3)/(3.*A(N_range)
                *numpy.asarray([H(N) for N in N_range])))))
    result = simps(func_int, N_range)

    return -(k1**2. +k2**2. +k3**2)/4.*result
    *numpy.array([0.+1.j], dtype=complex)

def calG_cc(hk_k1_array, hk_k2_array, hk_k3_array,
 k1, k2, k3, _Nics, _Nshss):
    '''Returns the value of the complex conjugate of \mathcal{G}
    which is in turn used to estimate G, the tensor bi-spectrum.
    The integral is evaluated for e-fold N ranging from _Nics till
    _Nshss. Note that the extra factor exp(-(e*k)/(A*H)) is put in
    by hand to satisfy the consistency relation.'''
    N_range = numpy.linspace(_Nics, _Nshss, len(hk_k1_array))
    func_int = ((A(N_range)/numpy.asarray([H(N) for N in N_range]))*
                (hk_k1_array*hk_k2_array*hk_k3_array)*
                (numpy.exp(-e*(k1 +k2 +k3)/(3.*A(N_range)
                *numpy.asarray([H(N) for N in N_range])))))
    result = simps(func_int, N_range)

    return (k1**2. +k2**2. +k3**2)/4.*result
    *numpy.array([0.+1.j], dtype=complex)

k1 = 1e-02
kmin = 1e-03
kmax = 1e-02
k3 = numpy.arange(0.,1.,.05)*k1

k_array = []
'''Since k1 is fixed, k_array will contain the set of [k2, k3] values.'''
for i in range(len(k3)):
    if k3[i]/k1 < 0.5:
        k2 = numpy.linspace(1. -k3[i]/k1, 1., 2 +int(k3[i]/k1/0.05))*k1
        [k_array.append([kx, k3[i]]) for kx in k2]
    else :
        k2 = numpy.linspace(k3[i]/k1, 1., 2 +int((1. -k3[i]/k1)/0.05))*k1
        [k_array.append([kx, k3[i]]) for kx in k2]

print len(k_array)
print k_array

hk_k1_array = numpy.empty(0, dtype=complex)
hk_k2_array = numpy.empty(0, dtype=complex)
hk_k3_array = numpy.empty(0, dtype=complex)
```

```
e =1./50

Nics = solve_Nics(kmin, N_array)
Nshss = solve_Nshss(kmax, N_array)

hk_k1_array = evolve_hk(k1, Nics, Nshss, step)
tps_k1 = 4.*(k1)**3./(2.*numpy.pi**2.)
*(numpy.absolute(hk_k1_array[-1]))**2.

def main(k_set):
    k2, k3 = k_set

    hk_k2_array = evolve_hk(k2, Nics, Nshss, step)
    hk_k3_array = evolve_hk(k3, Nics, Nshss, step)

    tps_k2 = 4.*(k2)**3./(2.*numpy.pi**2.)
    *(numpy.absolute(hk_k2_array[-1]))**2.
    tps_k3 = 4.*(k3)**3./(2.*numpy.pi**2.)
    *(numpy.absolute(hk_k3_array[-1]))**2.

    CalG = calG(hk_k1_array, hk_k2_array, hk_k3_array,
    k1, k2, k3, Nics, Nshss)
    CalG_cc = calG_cc(hk_k1_array, hk_k2_array,
    hk_k3_array, k1, k2, k3, Nics, Nshss)

    G = ((hk_k1_array[-1]*hk_k2_array[-1]*hk_k3_array[-1])*CalG
+(numpy.conj(hk_k1_array[-1])*numpy.conj(hk_k2_array[-1])
*numpy.conj(hk_k3_array[-1]))*CalG_cc)

    h_NL = -((4./(2.*numpy.pi**2.))**2.*(k1**3.*k2**3.*k3**3*G)/
             (2.*k1**3.*tps_k2*tps_k3 +2.*k2**3.*tps_k3*tps_k1
             +2.*k3**3.*tps_k1*tps_k2))

    print (k1, k2, k3, str(tps_k1).strip('[]'),
    str(tps_k2).strip('[]'), str(tps_k3).strip('[]'),
    str(CalG.real).strip('[]'), str(CalG.imag).strip('[]'),
    str(G.real).strip('[]'), str(G.imag).strip('[]'),
    str(h_NL.real).strip('[]'))

    return None

pool = mp.Pool(processes = 4)
temp_results =
[pool.apply_async(main, args = (k_set, )) for k_set in k_array[2:]]
results = []
```

```
for i in range(len(temp_results)):
        results.append(temp_results[i].get())

print results

CalG = calG(hk_k1_array, hk_k1_array, hk_k1_array,
k1, k1, k1, Nics, Nshss)
CalG_cc = calG_cc(hk_k1_array, hk_k1_array, hk_k1_array,
k1, k1, k1, Nics, Nshss)

G = ((hk_k1_array[-1]*hk_k1_array[-1]*hk_k1_array[-1])*CalG
+(numpy.conj(hk_k1_array[-1])*numpy.conj(hk_k1_array[-1])
*numpy.conj(hk_k1_array[-1]))*CalG_cc)

h_NL = -((4./(2.*numpy.pi**2.))**2.*(k1**3.*k1**3.*k1**3*G)/
        (2.*k1**3.*tps_k1*tps_k1 +2.*k1**3.*tps_k1*tps_k1
         +2.*k1**3.*tps_k1*tps_k1))

print (k1, k1, k1, str(tps_k1).strip('[]'),
str(CalG.real).strip('[]'), str(CalG.imag).strip('[]'),
str(G.real).strip('[]'), str(G.imag).strip('[]'),
str(h_NL.real).strip('[]'))
```